Università Ca' Foscari di Venezia
Dipartimento di Scienze Ambientali, Informatica e Statistica

Corso di Laurea Magistrale in Informatica - Computer Science

Tesi di laurea magistrale

Structural Signatures through Continuous-Time Quantum Walks with Decoherence

Candidato:
Gianpietro Basei
Matricola 810738

Relatore:
Prof. Andrea Torsello

Anno Accademico 2013–2014

ABSTRACT

Random walks have been used extensively to characterise the structures of complex graphs. Quantum walks are the analogue of classical random walks and have been recently used to study and develop quantum algorithms: unlike the classical case, where the evolution of the walk is governed by a stochastic matrix, in the quantum case the evolution is governed by a complex unitary matrix. Therefore quantum walks are non-ergodic and do not possess a limiting distribution. Recent approaches based on quantum walks have shown to achieve good results characterizing structures, since they avoid the over smoothing properties of their classical counterparts.

In quantum mechanics, decoherence represents the emergence of classical properties due to the interaction of the quantum system with the surrounding environment.

In this work we provide an overview of Quantum Computation and we study the effects of decoherence on Continuous-Time Quantum Walks to build a novel structural signature, the Decoherent Walk Signature, for characterising the nodes of a graph.

Our approach merges the wave-like transport of quantum walks with the diffusion process of classical walks, thus bringing the best of both worlds. The signature has been tested on both synthetic and real world graphs, exhibiting strong advantages over classical walks and marginal ones with respect to quantum walks.

CONTENTS

LIST OF FIGURES

LIST OF TABLES

1 BACKGROUND

1.1 INTRODUCTION

In this work we will provide an overview of Quantum Computation and we will study the effects of decoherence on Continuous-Time Quantum Walks to build a novel structural signature, the Decoherent Walk Signature, that merges the wave-like transport of quantum walks with the diffusion process of classical walks for characterising the nodes of a graph.

The document is organized as follows: first, in this chapter, we will introduce the concept of Feature Descriptor. Then we will give an overview on two of he main concepts that will be used in the thesis: the Hilbert spaces and the Laplace-Beltrami operator (and its discrete version, the graph Laplacian). Then we will briefly introduce the classical random walks.

Chapter 2, instead, is dedicated to Quantum Mechanics and Quantum Computation. In particular, we will give an overview on the main concepts that are used in Quantum Computation, we will introduce the quantum states and the quantum operators, giving an example of a very famous experiment, known as Young's experiment, that explains the concepts of quantum entanglement and quantum coherence. Then we will give a brief overview over quantum random walks, both in the discrete and continue settings.

In Chapter 3 we will describe the state of the art, focusing on two approaches that we are going to extend thanks to the structural signature described in Chapter 4.

Finally, in Chapter 5 we will present the results obtained applying our approach in both synthetic and real word graphs.

1.2 FEATURE DESCRIPTORS

The definition of a feature descriptor for characterizing points on a three dimensional shape, or in general on a graph, is a crucial task in many fields, such as 3D shape analysis, object recognition (an important example that falls into this category is face recognition), shape matching, shape segmentation and shape retrieval, clustering, robotics, 3D object databases, surface alignment, medical image analysis and molecular biology.

The goal is to associate to points (or nodes) a feature vector defined in a single or multi-dimensional feature space, which ideally contains all local and global information about the points that are relevant for the specific field of application. This data is usually computed for all of the nodes (or at least for the most significant

ones) and collected in a vector that is called *structural signature*[1] that is then made available for higher-level tasks.

It is of fundamental importance to choose what properties a signature has to capture. Some of the properties that the feature descriptor should fulfil, depending on the application, are:

Invariance The signature should be invariant (or at least insensitive) to transformations: isometric[2] and congruent[3] objects should have the same (or at least similar) signature. The signature should be independent from the object size, moreover the signature of a scaled object should be the same of the one of the original object.

Robustness Similar object should have similar signatures, moreover the signature should depend continuously from deformations of the object such as node insertion, node deletion and noise addition.

Discriminativity Although similar objects should have similar signatures, the resulting descriptor should be distinguishable.

Completeness Ideally, the signature should represent the object uniquely.

Efficiency The signature should be retrieved in a reasonable time.

Compression The signature should not be redundant, i.e. a part of it could not be computed starting from the rest of the data. Moreover the signature should be concise, still remaining informative.

Generality The signature should be independent from the application in which it will be used, moreover it would be desired its independence from of the representation of the object.

Intuitiveness It would be desired that the signature had a geometrical or physical interpretation.

Of course, in general it is necessary to find a trade-off between those properties, focusing on the ones that are fundamental for the specific task in which the signature will be used.

1.3 HILBERT SPACES

An Hilbert space is a generalization of the Euclidean space. Given a surface S, we denote as X the space of real-valued functions defined on the surface. The function

1 Structural signatures are also referred as *fingerprints*.

2 A mapping on a surface S into another surface $\tilde{S}$ is said to be isometric if the length of any arc on $\tilde{S}$ is the same of its inverse image on S. In other words, two objects are isometric if there exist an homeomorphism from one to the other (called isometry) that preserves geodesic distances.

3 Two objects are congruent if it is possible to transform them into each other by rigid motions or reflections.

space X is said to be complete[4] with respect to a norm if a sequence of functions $f_1, f_2, \ldots$ such that:

$$\lim_{n,m\to\infty} \|f_n - f_m\| = 0 \tag{1.1}$$

converge to X. In the case of the norm being defined as:

$$\|f\| = \sqrt{\langle f, f\rangle} \tag{1.2}$$

where $\langle\cdot,\cdot\rangle$ denotes the *inner product*[5], the function space is called *Hilbert space*. Hilbert spaces are usually denoted by $\mathcal{H}$.

One of the properties of Hilbert spaces is the possibility of defining function bases and project onto these bases using inner product: then using a basis φ_i a function f will be defined as:

$$f = \sum_i \alpha_i \varphi_i \tag{1.3}$$

if $\|\varphi_i\| = 1\ \forall i$, the basis is said to be orthonormal and hence $\langle\varphi_i, \varphi_j\rangle = 0\ \forall i \neq j$. Given the function f, then, it is possible to retrieve the coordinates α_i by projecting f onto the basis, formally $\alpha_i = \langle f, \varphi_i\rangle$.

1.4 THE LAPLACE-BELTRAMI OPERATOR

In this section will be remarked some useful concepts related to spectral graph theory that will be used in the thesis. First is presented the Graph Laplacian, then its continuous version is described. For a more detailed view on this topic one can refer to [Chung, 1997].

1.4.1 Discrete setting: Graph Laplacian

The *Graph Laplacian* (also known as Laplacian matrix or discrete Laplacian) of a given graph $G = (V, E)$ is defined as the matrix $L = D - A$, where A is the adjacency matrix of the graph G and D is the diagonal matrix whose diagonal elements are the sum of the elements in the corresponding row of the adjacency

4 A complete vector space is also called a *Banach space*.

5 The inner product, also known as dot product, between vectors $\mathbf{x}$ and $\mathbf{y}$ is defined as:

$$\langle \mathbf{x}, \mathbf{y}\rangle = \sum_i x_i y_i$$

A possible definition of an inner product among two functions f_1 and f_2 on a surface S is given by:

$$\langle f_1, f_2\rangle = \int_S f_1(x) f_2(x) \mathrm{d}x$$

matrix (formally, the elements d_u of the matrix D are defined as $d_u = \sum_{v \in V} A(u, v)$). This results in a matrix whose elements are:

$$L(i,j) = \ell_{i,j} = \begin{cases} -w_{i,j} & \text{if } (i,j) \in E \\ d_i & \text{if } i = j \\ 0 & \text{otherwise.} \end{cases} \tag{1.4}$$

where the coefficients $w_{i,j}$ are weights associated to the edges $(i,j) \in E$ and $d_i = \sum_{k \neq i} w_{i,k}$.

The *Normalized Laplacian*, denoted by $\mathcal{L}$, is instead defined as:

$$\mathcal{L}(i,j) = \tilde{\ell}_{i,j} = D^{-\frac{1}{2}} L D^{-\frac{1}{2}} = \begin{cases} -\frac{1}{\sqrt{d_i d_j}} & \text{if } (i,j) \in E \\ 1 & \text{if } i = j \text{ and } d_i \neq 0 \\ 0 & \text{otherwise.} \end{cases} \tag{1.5}$$

The first eigenvector of the the Graph Laplacian is the vector $(1, 1, \ldots, 1)^T$, and its associated eigenvalue is equal to 0. The second eigenvector is the so called *Fiedler vector*, and can be used to partition a graph or as permutation vector for numerical computations. Its associated eigenvalue represents the *algebraic connectivity* of the graph, and it is greater than zero if and only if the graph is connected. The number of eigenvalues equal to zero corresponds indeed to the number of connected components of the graph. The algebraic connectivity is dependent on the number of vertices, as well as the way in which vertices are connected, moreover it decreases with the number of vertices, and increases with the average degree.

The Fiedler vector can be also seen as a 1-dimensional embedding of G on a line, formally it can be seen as the solution of the following constrained minimization problem:

$$\begin{aligned} \underset{u}{\text{minimize:}} \quad & u^T L u \\ \text{subject to:} \quad & \sum_i u_i = 0 \text{ and } \sum_i u^2 = 1. \end{aligned} \tag{1.6}$$

Since the Graph Laplacian, by construction, is a symmetric matrix, its eigenvectors are orthogonal and so they can be used as a vector basis.

1.4.2 Continuous setting: Laplace-Beltrami

The *Laplace-Beltrami operator* (also referred as *LBO*) is the generalization of the Laplace operator to a manifold Ω, and it is defined as the divergence of the gradient of the scalar function $f : \Omega \to \mathbb{R}$:

$$\Delta_f = \operatorname{div}(\operatorname{grad}(f)) \tag{1.7}$$

also written:

$$\Delta_f = \nabla(\nabla f) \tag{1.8}$$

Commonly, in computer vision, it is defined as the negative of the divergence of the gradient of the scalar field. Its spectral components can be computed by solving the Helmholtz equation: $\Delta_f = -\lambda f$, where λ represents the eigenvalues. In particular, given the equation:

$$\Delta_f \phi = \lambda \phi \tag{1.9}$$

the scalar λ, represents the eigenvalue, while the vector ϕ is called a eigenvector or eigenfunction. Note that in the case of the Laplace-Beltrami operator (equivalently to the case of the discrete Laplacian), the eigenvalue $\lambda = 0$ is always a solution, and the corresponding eigenvector represents a constant function.

Since the Laplace-Beltrami operator is a positive self-joint operator, its eigen-decomposition give non-negative eigenvalues λ. Moreover, if we assume that the domain is compact, his spectrum is discrete ($0 < \lambda_1 < \lambda_2 < \dots$). Generally this is not the case, and the eigenvalues consists in a sequence $0 \leq \lambda_1 \leq \lambda_2 \leq \dots$. The number of times an eigenvalues is repeated is called the multiplicity of the eigenvalue.

The LBO is Hermitian[6], so the eigenfunctions corresponding to its different eigenvalues are orthogonal, thus the eigenfunctions provide a basis for the space of the functions defined on the manifold Ω.

The spectrum of the Laplace-Beltrami operator only depends on the gradient and on the divergence, and the gradient and the divergence depend on the Riemannian structure of the manifold: this implies that the LBO is isometric invariant. Moreover, scaling by a factor a results in scaled eigenvalues by a factor of $1/a^2$, and so, by normalizing the eigenvalues, the Laplace-Beltrami operator results to be scale invariant. Moreover, it can be proved that its spectrum has a continuous dependence on deformations. Hence, signatures based on the Laplace-Beltrami operator (or in its discrete formulation) are likely to possess these properties, that were described as desirable in Section 1.2.

Unfortunately, the spectrum of the Laplacian is not sufficient to determine all the features, even if geometrical and topological informations are contained in the eigenvalues, and there are cases where different objects results in the same spectrum (in this case they are said to be *isospectral*).

1.5 RANDOM WALKS

Given a graph $G = (V, E)$, and being G a connected graph with n nodes and m edges, a *random walk* on G (also called *drunken walk*) is defined as a stochastic process in which, starting from a node v_0, we move at each time $t = 0, 1, \dots$ in one of the nodes of the neighbourhood of the current node v_t with uniform probability (i.e. the probability of moving in one of the neighbours of v_t is equal to $1/d(v_t)$, where $d(x)$ is the degree of the node x, namely the number of vertex incident to x). The resulting sequence of nodes composing the walk is a Markov chain. Denoting

6 A linear operator A is said to be Hermitian if for each $f, g \in \mathcal{H}$ it holds that $\langle Af, g\rangle = \langle f, A^* g\rangle$. Eigenfunctions of Hermitian operators associated to different eigenvalues have real eigenvalues and are orthogonal.

as P_t the probability distribution of v_t ($P_x(t) = \Pr(v_t = x)$), we can define the generator matrix (note the similarity with Eq.(1.4)) of transition probabilities of the chain as follows:

$$M(i,j) = m_{i,j} = \begin{cases} 1 & \text{if } i \neq j, (i,j) \in E \\ -\frac{1}{d(i)} & \text{if } i = j \\ 0 & \text{else.} \end{cases} \tag{1.10}$$

so:

$$\frac{\mathrm{d}P_x(t)}{\mathrm{d}t} = -\sum_y M_{x,y} P_y(t) \tag{1.11}$$

If G is regular, then the chain is symmetric (the probability of moving from a node x to a node y is the same than moving from y to x), else for non-regular graphs this property is replaced by time reversibility: a random walk traveled backward is also a random walk, and the probability distribution of the backward walk is related to the one of the walk, in particular for every pair $x, y \in V$, $\pi(x)M_{x,y} = \pi(y)M_{y,x}$.

In general, the probability distributions $P(0), P(1), \ldots$ are different, but in the case that $P(1) = P(0)$ (and consequently $P(t) = P(0)$, $\forall t \geq 0$) the walk is said to be stationary (or steady-state). In particular, the unique stationary distribution for each graph is:

$$\pi(x) = \frac{d(x)}{2m} \tag{1.12}$$

It follows that, if G is regular, the uniform distribution on V is stationary.

A *continuous-time random walk* on a graph G models a Markovian process over the nodes of the graph, where the transactions are allowed only between nodes that are connected by an edge.

Denoting as $\mathbf{p}_t \in \mathbb{R}^n$ the state of the walk at time t, such that its i-th entry gives the probability of the walk being at vertex i at time t, then the state vector evolves according to:

$$\mathbf{p}_t = \mathrm{e}^{-Mt}\, \mathbf{p}_t \tag{1.13}$$

where M is the generator matrix of the Markovian process.

Classical random walks, both in discrete and continuous version, are often used to describe diffusion processes, in particular they have been widely studied in many fields such as informatics, physics, chemistry and economics to explain Markov processes observed in those fields.

For a detailed view on classical random walks and their properties, one can refer to [Lovász, 1993].

2 QUANTUM MECHANICS

Quantum mechanics provide a mathematical and conceptual framework for the development of physical theories of Quantum Physics. In quantum mechanics, the standard notion is the so called Dirac notation (also called *bra-ket notation*). The fundamental notations are presented in Table 2.1.

Notation	Description
z^*	Complex conjugate of $z \in \mathbb{C}$. $(i+1)^* = (1-i)$
$\|\psi\rangle$	A *ket*, represents a vector. This notation is used to indicate the state ψ. Note that ψ is a label that identify a state: any label can be used, but usually states are labeled by ψ and φ.
$\langle\psi\|$	A *bra*, represents the conjugate transpose of the corresponding ket $\|\psi\rangle$.
$\langle\varphi\|\psi\rangle$	Inner product between vectors $\|\varphi\rangle$ and $\|\psi\rangle$.
$\|\varphi\rangle \otimes \|\psi\rangle$	Tensor product between vectors $\|\varphi\rangle$ and $\|\psi\rangle$ can also be written with the abbreviate notations $\|\varphi\rangle\|\psi\rangle$, $\|\varphi, \psi\rangle$ and $\|\varphi\psi\rangle$.
A^*	Complex conjugate of the matrix A: $\begin{bmatrix} a & b \\ c & d \end{bmatrix}^* = \begin{bmatrix} a^* & b^* \\ c^* & d^* \end{bmatrix}$
A^T	Transpose of the matrix A: $\begin{bmatrix} a & b \\ c & d \end{bmatrix}^T = \begin{bmatrix} a & c \\ b & d \end{bmatrix}$
$A^\dagger$	Hermitian conjugate (or adjoint) of the matrix A: $\begin{bmatrix} a & b \\ c & d \end{bmatrix}^\dagger = \begin{bmatrix} a^* & c^* \\ b^* & d^* \end{bmatrix}$ Corresponds to $A^\dagger = (A^T)^*$.
$\langle\varphi\|A\|\psi\rangle$	Inner product between $\|\varphi\rangle$ and $A\|\psi\rangle$, equivalently inner product between $A^\dagger\|\varphi\rangle$ and $\|\psi\rangle$.

Table 2.1: Summary of the most important notations in quantum mechanics. This notation is known as Dirac notation or bra-ket notation

2.1 QUANTUM SYSTEMS AND QUANTUM STATES

Considering a finite Hilbert space $\mathcal{H}$ with an orthonormal[1] set of basis states $|s\rangle,\ s \in \Omega$, the states can be interpreted as the possible classical states of the system described by the Hilbert space.

The state of the system $|\psi\rangle$ is an unit vector in $\mathcal{H}$ which completely describes the state space of the system and can be written as:

$$|\psi\rangle = \sum_{s\in\Omega} \alpha_s |s\rangle \tag{2.1}$$

where α_s is the *amplitude*[2], and $\alpha \in \mathbb{C},\ |\psi\rangle \in \mathbb{C}^{|\Omega|}$.

The simplest quantum mechanical system is the *qubit*, which has a two dimensional state space. An orthonormal set of basis states for the state space can be defined by the states[3] $|0\rangle$ and $|1\rangle$, then a state vector for this system can be written as:

$$|\psi\rangle = a|0\rangle + b|1\rangle \tag{2.2}$$

where $a, b \in \mathbb{C}$. The condition $\langle\psi|\psi\rangle = 1$ (i.e.: the state vector is an unit vector), sometimes called *normalization condition*, is therefore equivalent to $|a|^2 + |b|^2 = 1$.

The main difference that one can notice between bits and qubits is in the fact that for qubits can hold a *superposition* of the states $|0\rangle$ and $|1\rangle$ of the form $a|0\rangle + b|1\rangle$. In general any linear combination $\sum_i \alpha_i|\psi_i\rangle$ is a superposition for the state $|\psi\rangle$ of states $|\psi_i\rangle$ with amplitude α_i. So for example the state

$$\frac{|0\rangle - |1\rangle}{\sqrt{2}} \tag{2.3}$$

is a superposition of the two basic states with amplitude $1/\sqrt{2}$ for state $|0\rangle$ and $-1/\sqrt{2}$ for state $|1\rangle$.

The two main operations on a quantum system are *evolution* and *measurement*, and will be discussed in the next two subsections.

2.1.1 Evolution of a Quantum System

The evolution in time of a closed quantum system is described by *unitary transformations*, that is, the state of the system $|\psi\rangle$ at time t_i is related to the state of the system $|\psi'\rangle$ at time t_{i+1} by an unitary operator U ($UU^\dagger = I$) which is dependent only on times t and t_{i+1}:

$$|\psi'\rangle = U|\psi\rangle \tag{2.4}$$

1 A set $|i\rangle$ of vectors with index i is orthonormal if each vector is a unit vector (i.e.: it has unitary norm), and distinct vectors in this set are orthogonal (i.e.: $\langle i|j\rangle = \delta_{ij}$).

2 The amplitude α_s for a quantum state $|s\rangle$ is a complex number whose modulus squared represents a probability or a probability density, where $\alpha_s\alpha_s^* \in [0, 1]$ and in a closed system $\sum_s \alpha_s\alpha_s^* = 1$.

3 Intuitively, those states corresponds to the values 0 and 1 that a bit can take, this is the motivation behind the name "qubit".

Unitary transformations preserve norms, can be diagonalized with an orthonormal set of eigenvectors and the corresponding eigenvalues are of absolute value 1.

Quantum mechanics does not define what the state space of a particular quantum system is, nor it defines which operators U describes real world quantum dynamics, but it assures that the evolution of any closed quantum system can be described in a way similar to the one in Eq.(2.4). Note that in the case of qubits, any unitary operator can be realized in realistic systems. Note also that is required that the system being described is not interacting with other systems: this is not the case in real world, since all the systems are interacting with other systems (for example with the surrounding environment), but it is also true that in principle every open system can be described as part of a larger closed system (the Universe) which is undergoing unitary evolution.

We can describe the evolution of quantum systems in the continuous time. The time evolution of the state $|\psi\rangle$ of a closed quantum system is described by the *Schrödinger equation*:

$$i\hbar\frac{\mathrm{d}|\psi\rangle}{\mathrm{d}t} = H|\psi\rangle \tag{2.5}$$

where H is a Hermitian operator known as the *Hamiltonian*[4] and $\hbar$ is the *reduced Planck's constant*[5]. If we know the Hamiltonian of a system, then in principle we can understand the complete dynamic of such system. As it is clear, in general the task to define the better Hamiltonian to describe the evolution of a quantum system is very difficult and has to be addressed by physical theories.

Recall the spectral decomposition theorem:

Theorem 1 (Spectral Decomposition)**.** *Any normal operator A ($AA^\dagger = A^\dagger A$) on a vector space V is diagonal with respect to some orthonormal basis for V. Conversely, any diagonalizable operator is normal.*
In other words, A can be written as:

$$A = \sum_i \lambda_i |i\rangle\langle i|$$

where λ_i are the eigenvalues of A, $|i\rangle$ is an orthonormal basis for V, and each $|i\rangle$ is an eigenvector of A with eigenvalue λ_i.
It is also possible to write A in terms of projectors:

$$A = \sum_i \lambda_i P_i$$

4 In Quantum Mechanics, the Hamiltonian is the operator that describes the total energy of the system. It is related to the time-evolution of the system, since is spectrum represents the set of possible outcomes when the total energy is measured.

5 The Planck's constant h is a physical constant representing the quantum of action that express the relationship between energy and frequency, known as the Planck–Einstein relation, $E = h\nu$, where E is the energy and ν is the frequency of its associated electromagnetic wave. The normalized version $\hbar = h/2\pi$ of the Planck's constant, called the reduced Planck's constant, represents the quantization of the angular momentum. The value of this constant has to be determined experimentally. It is a common practice, while dealing with the Schrödinger equation, to absorb this constant into the Hamiltonian H thus setting $\hbar = 1$.

where λ_i are the eigenvalues of A and P_i is the projector onto the λ_i eigenspace of A.

Since the Hamiltonian is ah Hermitian operator, it has a spectral decomposition of the form:

$$H = \sum_E E|E\rangle\langle E| \tag{2.6}$$

where E are the eigenvalues and $|E\rangle$ the corresponding eigenvectors. We refer to the states $|E\rangle$ as energy states for the system, while we refer to E as the energy for the state $|E\rangle$. The lowest energy (i.e.: the smallest eigenvalue) is often called the *ground state energy* for the system, and the corresponding eigenstate is called *ground state*.

The states $|E\rangle$ are often called *stationary states* because their only change in time is to acquire an overall numerical factor:

$$|E\rangle \to \exp\left(\frac{-iEt}{\hbar}\right)|E\rangle \tag{2.7}$$

The connection between Eq.(2.5) and Eq.(2.4) holds in the fact that if we define:

$$U(t_i, t_{i+1}) \equiv \exp\left(\frac{-iH(t_1, t_{i+1})}{\hbar}\right) \tag{2.8}$$

then:

$$|\psi(t_{i+1})\rangle = \exp\left(\frac{-iH(t_1, t_{i+1})}{\hbar}\right)|\psi(t_i)\rangle = U(t_i, t_{i+1})|\psi(t_i)\rangle \tag{2.9}$$

and it can be proved that the operator $U(t_i, t_{i+1})$ is unitary and furthermore any unitary operator U can be realized in the form $U = \exp(iK)$ for some Hermitian operator K. Hence there is a one-to-one correspondence between the discrete-time description of dynamics using unitary operators and continuous time description of dynamics using Hamiltonians.

2.1.2 Quantum measurement

Quantum measurements are described as a collection $\{M_m\}$ of *measurement operators* acting on the state space of the quantum system being measured, where m indicates a possible outcome for the system.

Immediately before a measurement, if the system is on the state $|\psi\rangle$, the probability that the m occurs is equal to:

$$\Pr(m) = \langle\psi|M_m^\dagger M_m|\psi\rangle \tag{2.10}$$

and after the measurement the state become:

$$|\psi'\rangle = \frac{M_m|\psi\rangle}{\sqrt{\langle\psi|M_m^\dagger M_m|\psi\rangle}} \tag{2.11}$$

Note that if the states $|\psi_i\rangle$ are not orthonormal, it is not possible to distinguish them.

Measurement operators satisfies the so called *completeness equation*, that states:

$$\sum_m M_m^\dagger M_m = I \tag{2.12}$$

A direct implication of the completeness equations is that the probabilities of the measurements sum to one, as if the following equation is satisfied for all $|\psi\rangle$ it is equivalent to the completeness equation:

$$\sum_m \Pr(m) = \sum_m \langle\psi|M_m^\dagger M_m|\psi\rangle = 1 \tag{2.13}$$

Coming back to the example of the qubits and defining the two measurement operators as $M_0 = |0\rangle\langle 0|$ and $M_1 = |1\rangle\langle 1|$, we can note that since the two operators are Hermitian and $M_0^2 = M_0,\ M_1^2 = M_1$, the completeness equation is obeyed since $M_0 + M_1 = M_0^\dagger M_0 + M_1^\dagger M_1 = I$.

Supposing that the state $|\psi\rangle = a|0\rangle + b|1\rangle$ is being measured, the probability to obtain the outcome 0 after a measurement is then:

$$\Pr(0) = \langle\psi|M_0^\dagger M_0|\psi\rangle = \langle\psi|M_0|\psi\rangle = |a|^2 \tag{2.14}$$

while the probability to obtain the outcome 1 after a measurement is:

$$\Pr(1) = \langle\psi|M_1^\dagger M_1|\psi\rangle = \langle\psi|M_1|\psi\rangle = |b|^2 \tag{2.15}$$

Hence the state after the measurement is:

$$|\psi'\rangle = \begin{cases} \frac{M_0|\psi\rangle}{|a|} = \frac{a}{|a|}|0\rangle = |0\rangle & \text{if we obtain 0 as outcome,} \\ \frac{M_1|\psi\rangle}{|b|} = \frac{b}{|b|}|1\rangle = |1\rangle & \text{if we obtain 1 as outcome.} \end{cases} \tag{2.16}$$

Note that the multipliers like $a/|a|$ have been omitted, the reason holds in the fact that from an observational point of view, the states $|0\rangle,\ |1\rangle$ are the same as $(a/|a|)|0\rangle,\ (b/|b|)|1\rangle$. In fact, in general we say that the state $\mathrm{e}^{i\theta}|\psi\rangle$, where $|\psi\rangle$ is a state vector and θ is a real number, is equal to the state $|\psi\rangle$ upto a global phase factor $\mathrm{e}^{i\theta}$. The statistics of measurements for these two states are identical, as for an outcome m the probabilities are:

$$\langle\psi|\,\mathrm{e}^{-i\theta}\,M_m^\dagger M_m\,\mathrm{e}^{i\theta}|\psi\rangle = \langle\psi|M_m^\dagger M_m|\psi\rangle \tag{2.17}$$

Hence, we can ignore global phase factor. This is not the case when each of the amplitudes of two states in some basis is related to a phase factor, in this case we say two states differ by a relative phase, and the measurements statistics for these two states are different, so it is not possible to refer to those states as equivalent.

There are two special cases of the measurement operation that are very important in literature: *projective measurements*, also known as Von Neumann measurements, and *positive operator-valued measurements*, which are referred with the acronym POVM.

A projective measurement is described by an Hermitian operator M, the observable, which spectral decomposition is:

$$M = \sum_m m P_m \tag{2.18}$$

where P_m is the projector onto the eigenspace of the operator with eigenvalue m. The possible outcomes corresponds to the eigenvalues m of the observable. Being at the state $|\psi\rangle$, the probability of measuring m is then $\Pr(m) = \langle\psi|M|\psi\rangle$, and the state after the measurement of m is $|\psi'\rangle = (P_m|\psi\rangle)/\sqrt{\Pr(m)}$. For projective measurements it is easy to calculate the expected value:

$$\langle M\rangle \equiv \mathrm{E}[M] = \sum_m m \Pr(m) = \langle\psi|M|\psi\rangle \tag{2.19}$$

From this follows the formulation of standard deviation associated to M:

$$\sigma_M = \sqrt{\langle M^2\rangle - \langle M\rangle^2} \tag{2.20}$$

Given two observables A and B, and setting up a large number of quantum systems in identical states $|\psi\rangle$ and then performing measurements of A on some of those systems and of B in others, then:

$$\sigma_A \sigma_B \geq \frac{|\langle\psi|[A,B]|\psi\rangle|}{2} \tag{2.21}$$

This is called the *Heisenberg uncertainty principle*[6].

For some applications the state of the system is of poor interest, while it is more interesting to study the probabilities of the measurement outcomes. This is for example the case of an experiment where the system is measured only after the conclusion of the experiment. In such cases the POVM measurements are widely used. Suppose to define:

$$E_m \equiv M_m^\dagger M_m \tag{2.22}$$

E_m is a positive operator, $\sum_m E_m = I$ and $\Pr(m) = \langle\psi|E_m|\psi\rangle$. The complete set of operators $\{E_m\}$ (called POVM) is sufficient to determine the probabilities of different measurement outcomes.

2.1.3 Composite states

Having two systems A and B defined in the Hilbert spaces $\mathcal{H}_A$ and $\mathcal{H}_B$, where the basis states for the two systems are respectively $|\psi\rangle$ and $|\varphi\rangle$, then the joint system is described by $\mathcal{H}_A \otimes \mathcal{H}_B$, and its base state is $|\psi\rangle \otimes |\varphi\rangle$. This indicates that the

6 Often the uncertainty principle is formulated as:

$$\Delta_x \Delta_{p_x} \geq \frac{\hbar}{2}$$

Refer to [Auletta et al., 2009] for a characterization of this principle.

set of basis states of the combined systems is spanned by al possible configurations of the two classical systems. More generally, the space of a composite physical system is the tensor product of the state space of the physical systems composing it ($|\psi_1\rangle \otimes |\psi_2\rangle \otimes \cdots \otimes |\psi_n\rangle$).

Composite states enable to define one of the most important and striking concepts of quantum mechanics: the concept of *quantum entanglement*. An entangled state is a state of a composite system whose subsystems are not probabilistically independent. In other words, a state of a composite system is entangled if it can not be written as a product of states of its components. Formally, two systems A and B are said to be entangled if their total state $|\psi\rangle_{AB}$ cannot be written in a factorized form as $|\psi\rangle_A \otimes |\psi\rangle_B$ for any basis. Note that this concept is different from the one of *quantum superposition* of states, which says that if for a system there exists two states $|x\rangle$ and $|y\rangle$ then also $\alpha|x\rangle + \beta|y\rangle$ (where $|\alpha|^2 + |\beta|^2 = 1$) is a state for the system. Entanglement implies superposition, but a superposition state is not necessarily entangled.

2.2 MIXED STATES AND DENSITY MATRICES

Up to this point, we have referred as states using vectors. The more general formulation involves the so called *density matrix*, that is mathematically equivalent to the concept of state vector, but is a much more powerful tool. The density matrix are generally used for describing quantum systems whose state is not known, or to describe subsystems of a composite quantum system. This second application is out of the scope of this thesis and will not be presented in this document, one can refer to [Nielsen and Chuang, 2011] for a more exhaustive view.

Given an ensemble of pure states[7] $|\psi_i\rangle$, each associate with a probability p_i, that is denoted by $\{p_i, |\psi_i\rangle\}$, we define the density operator for this system by the density matrix:

$$\rho \equiv \sum_i p_i |\psi_i\rangle\langle\psi_i| \tag{2.23}$$

Then, when the system is in a pure state $|\psi\rangle$, its density operator is simply:

$$\rho = |\psi\rangle\langle\psi| \tag{2.24}$$

Note that different ensembles of quantum states may result in the same density matrix.

A simple criterion to determine whether a system is in a pure or in a mixed state is to check if the trace[8] of the square of its density matrix is equal to one (in this case the system is in a pure state) or if it is less than one (in this case the system is in a mixed state).

7 A quantum system whose state $|\psi\rangle$ is known exactly is said to be in a *pure state*, otherwise it is said to be in a *mixed state*, or equivalently it is said to be in a *mixture of pure states*.

8 The trace of a matrix A is defined as the sum of its diagonal elements: $\mathrm{tr}(A) = \sum_i A_{ii}$. The trace is cyclic ($\mathrm{tr}(AB) = \mathrm{tr}(BA)$), linear ($\mathrm{tr}(A+B) = \mathrm{tr}(A) + \mathrm{tr}(B)$, $\mathrm{tr}(zA) = z\,\mathrm{tr}(A)$) and invariant under the unitary similarity transformation, since $\mathrm{tr}(UAU^\dagger) = \mathrm{tr}(UU^\dagger A) = \mathrm{tr}(A)$.

Density operators are characterized by the following theorem (for the proof one can refer to [Nielsen and Chuang, 2011]:

Theorem 2 (Characterization of density operators)**.** *Given an ensemble of states $|\psi_i\rangle$ each associated with a probability p_i (denoted by $\{p_i, |\psi_i\rangle\}$), an operator ρ is a density operator if and only if:*

- $\mathrm{tr}(\rho) = 1$
- *ρ is a positive operator.*

Similarly to vector states, if the system is initially in the state ψ_i with probability p_i and evolves according to an unitary operator U, then after the evolution the system will be in the state $U|\psi_i\rangle$. The new density matrix after the evolution will be:

$$\rho' = \sum_i p_i U|\psi_i\rangle\langle\psi_i|U^\dagger = U\rho U^\dagger \tag{2.25}$$

Supposing that the system is in an initial state $|\psi_i\rangle$, and supposing to perform a measurement described by the operator M_m, then the probability of obtaining the outcome m is:

$$\Pr(m|i) = \langle\psi_i|M_m^\dagger M_m|\psi_i\rangle = \mathrm{tr}(M_m^\dagger M_m|\psi_i\rangle\langle\psi_i|) \tag{2.26}$$

The last equality holds because for an arbitrary operator A given a unit vector $|\psi\rangle$, it holds that $\mathrm{tr}(A|\psi\rangle\langle\psi|) = \langle\psi|A|\psi\rangle$. Thus, the probability of getting the outcome m is:

$$\begin{aligned}\Pr(m) &= \sum_i \Pr(m|i)p_i \\ &= \sum_i p_i \,\mathrm{tr}(M_m^\dagger M_m|\psi_i\rangle\langle\psi_i|) \\ &= \mathrm{tr}(M_m^\dagger M_m \sum_i p_i|\psi_i\rangle\langle\psi_i|) \\ &= \mathrm{tr}(M_m^\dagger M_m \rho)\end{aligned} \tag{2.27}$$

It is easy to show that the density operator after obtaining m as outcome is:

$$\rho' = \sum_i p_i \frac{M_m|\psi_i\rangle\langle\psi_i|M_m^\dagger}{\mathrm{tr}(M_m^\dagger M_m\rho)} = \frac{M_m\rho M_m^\dagger}{\mathrm{tr}(M_m^\dagger M_m\rho)} \tag{2.28}$$

We can also reformulate the concept of composite state considering a set of systems each defined with a density matrix ρ_i: the state space of the composite system is the tensor product of the state space of its components, and then the state of the composite system is $\rho_1 \otimes \rho_2 \otimes \cdots \otimes \rho_n$.

2.3 EXAMPLES OF QUANTUM COMPUTATION

In the following will be presented an examples of quantum computation and application of quantum operators: the Young's experiment.

The original version of this experiment was performed at the beginning of the nineteenth century by the physicist Thomas Young to proof that the light behave as waves. The experiment consists in placing a light source, with a panel in front of it. Imagine to open two slits in this plane, named $S1$ and $S2$, and to place behind the panel a detector that captures the incoming light.

First, we want to study what happens when only a slit is open: the situation is presented in Figure 2.1, where we opened $S1$ and left $S2$ closed and in Figure 2.2, where we opened the slite $S2$ and left closed $S2$.

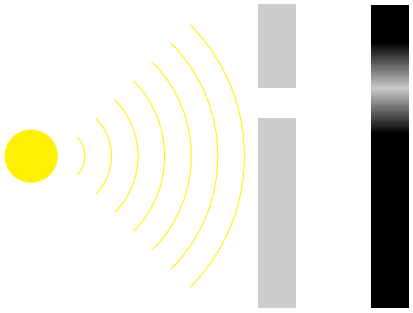

Figure 2.1: The Young's experiment: only slit $S1$ opened.

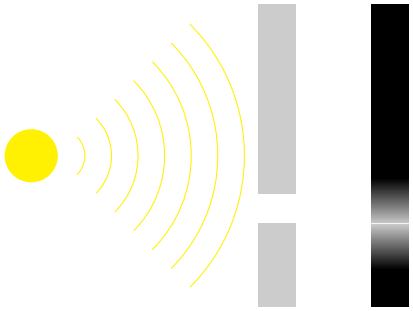

Figure 2.2: The Young's experiment: only slit $S2$ opened.

As we can see in Figure 2.1 and Figure 2.2, the pattern of the light detected follows a probability distribution expected by discrete particles.

If, instead, we open both the slits, the resulting pattern follows a typical interference pattern obtained with waves, and not the sum of the patterns for the two slits, as we can see in Figure 2.3. Moreover, when both slits are open, light do not appear in great quantity in areas where previously did, and a large quantity of light arrives in areas where previously did not.

After this experiment Thomas Young concluded that light behave like wave.

A natural question that arises is what happens if we use a coherent light source (like a laser), "shooting" one photon at time. The set up of this experiment is similar to the classical Young experiment, but this time we want to discretize the detector

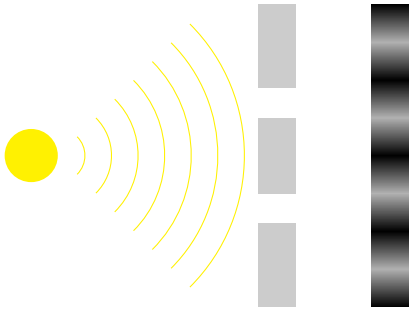

Figure 2.3: The Young's experiment: two slits open. Interference patterns typical of wave behaviour appears on the detector.

and we want to build an histogram representing the probability distribution of a photon to hit the i-th slot of the detector.

The first two experiments, produces similar distributions as the ones of the original Young's experiment, as we can see in Figure 2.4 and Figure 2.5.

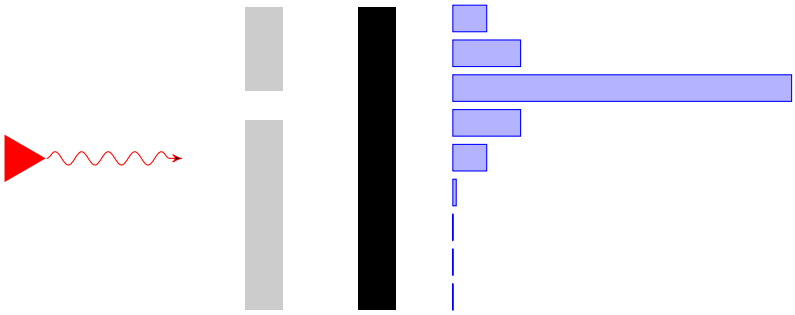

Figure 2.4: The Young's experiment: a single photon is shoot. Only $S1$ open.

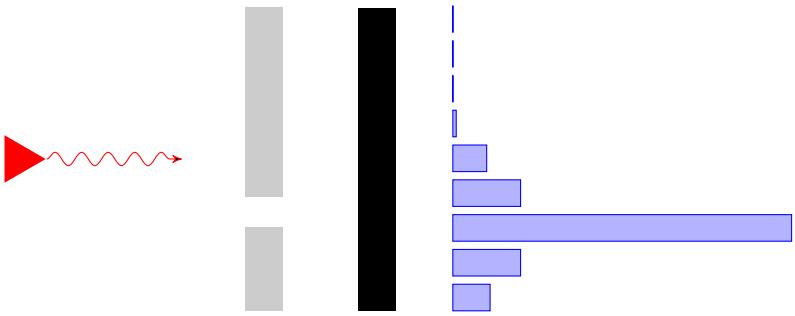

Figure 2.5: The Young's experiment: a single photon is shoot. Only $S2$ open.

The surprisingly result is that also in the case of the two slits open the resulting probability distribution obtained shooting one photon at time is the same that we obtained in the original Young's experiment, as we can see in Figure 2.6. This, indeed, means that photons interfere with themselves.

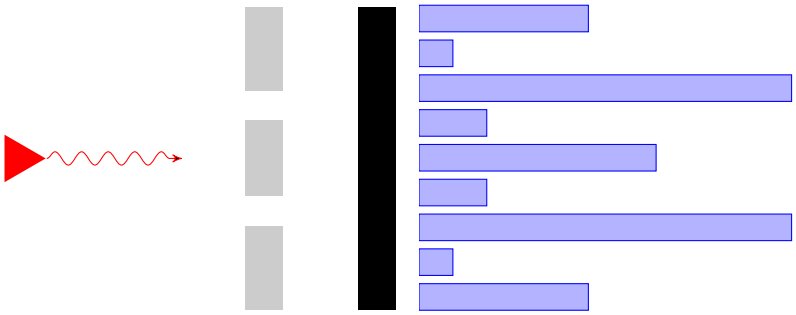

Figure 2.6: The young experiment: two slits open. The photon interfere with itself.

Let us perform another experiment: we put a spin in the first slit, in order to check whether the photon passed in the upper slit or in the lower slit. The puzzling result is that doing so the interference phenomena disappear, as we can see in Figure 2.7, and the probability distribution obtained is equal to the sum of the two probability distributions obtained in the experiments presented in Figures 2.4 and 2.5.

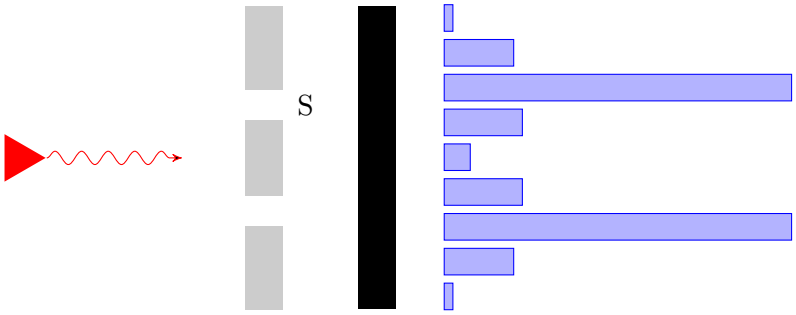

Figure 2.7: The young experiment: adding the spin (the system is thus entangled with the spin) the interference pattern disappeared.

The interpretation of this experiment is that light is neither particle nor wave, and, in general, experiments can demonstrate particle (photon) or wave properties, but not both at the same time. This concept is also referred as *Bohr's Complementarity Principle*.

Thanks to quantum mechanics we can formally describe this experiment and explain why the interference disappear. Let us first formalize the situation in absence of the spin (Figure 2.6).

We can use the states $|u\rangle$ and $|v\rangle$, where $|u\rangle$ describes the system when the photon passes in the upper slit and then arrives in the i-th slot of the detector:

$$|u\rangle = \sum_i u_i |i\rangle \tag{2.29}$$

and $|d\rangle$ describes the system when the photon passes in the lower slit and arrives in the i-th slot:

$$|d\rangle = \sum_i d_i |i\rangle \tag{2.30}$$

Hence, the state of the system can be written as:

$$\begin{aligned} |\psi\rangle &= \alpha|u\rangle + \beta|d\rangle \\ &= \sum_i (\alpha u_i + \beta d_i)|i\rangle \end{aligned} \tag{2.31}$$

The probability that the photon reaches the slot i is then:

$$\Pr(i) = |P_i\psi|^2 = \langle\psi|P_i|\psi\rangle \tag{2.32}$$

Let us project this state on i using the position operator $P_i = |i\rangle\langle i|$. This results in:

$$\begin{aligned} \Pr(i) &= \langle\psi||i\rangle\langle i||\psi\rangle \\ &= \left(\sum_j (\alpha^* u_j^* + \beta^* d_j^*)\langle j|\right)|i\rangle\langle i|\left(\sum_k (\alpha u_k + \beta d_k)|k\rangle\right) \\ &= (\alpha^* u_i^* + \beta^* d_i^*)(\alpha u_i + \beta u_i) \\ &= \alpha^*\alpha u_i^* u_i + \beta^*\beta d_i^* d_i + \alpha^*\beta u_i^* d_i + \alpha\beta^* u_i d_i^* \end{aligned} \tag{2.33}$$

Now consider the example in Figure 2.7: we need to add to our system the spin, which can be in the state $|\uparrow\rangle$, if the particle has not passed in the upper slit, or in the state $|\downarrow\rangle$, if the particle has passed in the upper slit, activating the spin. The states, hence, are:

$$|u,\downarrow\rangle = \sum_i u_i|u_i,\downarrow\rangle \tag{2.34}$$

where $|u,\downarrow\rangle$ describes the system when the photon passes in the upper slit activating the spin and then arrives in the i-th slot of the detector. Conversely, $|d,\uparrow\rangle$ describes the system when the photon passes in the lower slit (not activating the spin) and then arrives in the i-th slot of the detector:

$$|d,\uparrow\rangle = \sum_i d_i|d_i,\uparrow\rangle \tag{2.35}$$

Hence the initial state is no more separable, since it is entangled with the state of the spin:

$$\begin{aligned} |\psi\rangle &= \alpha|u,\downarrow\rangle + \beta|d,\uparrow\rangle \\ &= \sum_i (\alpha u_i|i,\downarrow\rangle + \beta d_i|i,\uparrow\rangle) \end{aligned} \tag{2.36}$$

We define the projectors as:

$$P_i = |i,\uparrow\rangle\langle i,\uparrow| + |i,\downarrow\rangle\langle i,\downarrow| \tag{2.37}$$

Then the probability that the photon reaches the slot i is:

$$\begin{aligned}\Pr(i) &= \langle\psi||i\rangle\langle i||\psi\rangle \\ &= \left(\sum_j (\alpha^* u_j^* \langle j,\downarrow| + \beta^* d_j^* \langle j,\uparrow|)\right) P_i \left(\sum_k (\alpha u_k |k,\downarrow\rangle + \beta d_k |k,\uparrow\rangle)\right) \\ &= (\alpha^* u_i^* \langle i,\downarrow| + \beta^* d_i^* \langle i,\uparrow|)(|i,\uparrow\rangle\langle i,\uparrow| + |i,\downarrow\rangle\langle i,\downarrow|)(\alpha u_i |i,\downarrow\rangle + \beta d_i |i,\uparrow\rangle) \\ &= \alpha^*\alpha u_i^* u_i + \beta^*\beta d_i^* d_i\end{aligned} \tag{2.38}$$

Note that the term $\alpha^*\beta u_i^* d_i + \alpha\beta^* u_i d_i^*$, that describes the interference of the photon with himself, is no more present.

This explains formally the double slit experiment: the interference disappears because the state of the particle is entangled with the spin. Every time we perform a measurement that let us known the state of the system, we destroy the superposition of states in the system and hence the interference disappears.

2.4 QUANTUM RANDOM WALKS

The term *Quantum Random Walk* was coined by [Y. Aharonov et al., 1993] illustrating the behaviour of a particle on a line, whose possible position is described by a wave packet $|\psi_{x_0}\rangle$ localized around a position x_0.

Similar to Classical Random Walks, a Quantum Random Walk is defined as a dynamical process over the vertices of a graph. However, instead of being characterized by a real vector that describes its evolution, the Quantum Walk is characterized by a complex-value amplitude vector, with no restrictions on sign or phase. This allows different path of the walks to interfere with each other, in constructive or destructive ways. Furthermore, the evolution Classical Random Walks is governed, as we explained in Chapter 1, by a stochastic matrix, while in the case of the Quantum Random Walk this matrix is replaced by a complex unitary matrix. This makes the Quantum Walk reversible, and its reversibility implies that the Quantum Walk is non-ergodic and do not posses a limiting distribution. This lack of convergence makes the Quantum Walks harder to study than Classical Random Walks.

Starting from the idea of quantum random walks, [Farhi and Gutmann, 1998] provided an algorithm that used quantum random walks to move through decision trees. Thanks to the framework provided by this work, many other approaches to Quantum Random Walks have been proposed. In particular, two models of Quantum Walks have been proposed: the discrete model and the continuous model. In the next subsections these approaches will be reviewed.

2.4.1 Quantum Random Walks for Decision Trees

As well illustrated in [Farhi and Gutmann, 1998], any computational problem can be solved by reformulating it in terms of decision trees, then usually a random walk is run on this tree, starting from the root and checking whether the tree contains or

not a node x at a distance of n levels from the root. A graphical example of such a tree is presented in Figure 2.8.

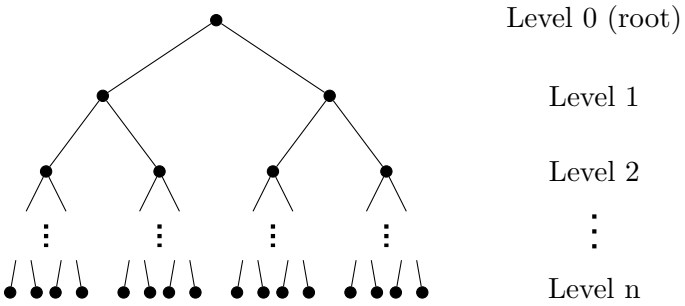

Figure 2.8: An example of decision tree: at level m there are 2^m nodes.

Usually, some of the nodes are eliminated because of the constraints imposed by the problem that is expressed by the decision tree. In this case, also the branch starting from that node is eliminated. An example of a decision tree in which some nodes have been removed due to the constraints imposed by the problem is presented in Figure 2.9.

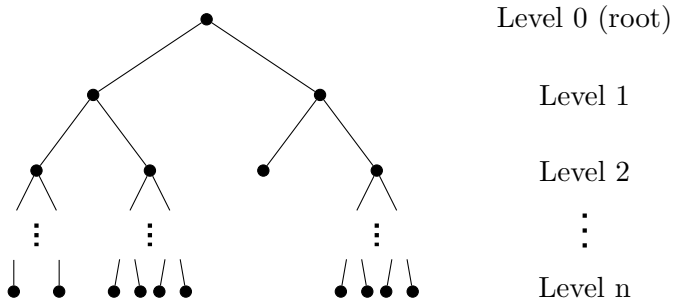

Figure 2.9: An example of decision tree in which some branches have been removed because of the constraints imposed by the problem: at level m there are now at most 2^m nodes.

The idea introduced by [Farhi and Gutmann, 1998] is to build a correspondence between nodes and quantum states, thus obtaining a basis for the Hilbert space. An Hamiltonian H with non-zero off-diagonal elements only where states (corresponding to nodes) are connected in the tree is constructed, then the system is started in correspondence of the root of the tree, then the system evolves according to:

$$U(t) = \mathrm{e}^{-iHt} \tag{2.39}$$

At any time t we can express the pure state as a superposition of basis states, then giving the initial state is possible to determine the probability of the system to be at the n^{th} level.

Being γ the fixed and time-independent probability to move to a connected node, they defined the Hamiltonian as:

$$\langle y|H|x\rangle = \begin{cases} \gamma d(x) & \text{if } x = y \\ -\gamma & \text{if } x \neq y,\ x \sim y \\ 0 & \text{if } x \neq y,\ x \nsim y. \end{cases} \tag{2.40}$$

Note that this definition is almost identical to the definition of the generator matrix in Eq.(1.10), since the nodes in a binary decision tree can be connected at most to 3 nodes (the father and two children).

Being $p_{y,x}(t)$ the classical probability to go from node x to node y in time t, as [Farhi and Gutmann, 1998] shown, similarly to Eq.(1.11) for $p_{y,x}(t)$ holds that:

$$\frac{\mathrm{d}}{\mathrm{d}t}p_{y,x}(t) = -\sum_z \langle y|H|x\rangle p_{z,x}(t) \tag{2.41}$$

The solution of the above differential equation is (one can note the similarity with Eq.(1.13)):

$$p_{y,x}(t) = \langle y|\, \mathrm{e}^{-Ht}|x\rangle \tag{2.42}$$

Then, using the same Hamiltonian, they proposed to let the system quantum mechanically evolve through the tree. They show that, being:

$$\alpha_{y,x}(t) = \langle y|\, \mathrm{e}^{-iHt}|x\rangle \tag{2.43}$$

the quantum amplitude to be found at y after a time t and starting from x, the probability is given by $|\alpha y, x(t)|^2$, with $\sum_y |\alpha y, x(t)|^2 = 1$ as a consequence of the fact that H by definition is Hermitian[9].

[Farhi and Gutmann, 1998] defined the family of three that are penetrable as the family of three for it is true that in a polynomial time the probability of reaching the n^{th} level is at worst polynomially small, and shown that any family of tree that are classically penetrable then they are quantum penetrable, furthermore they shown that there exists family of threes that are not classically penetrable but are quantum penetrable.

2.4.2 Discrete-Time Quantum Random Walks

The most studied model of Quantum Walk is the Discrete-Time Quantum Walk- which is also referred as *coined walk*, because a quantum coin is used to describe the dynamic of the walk, in order to make it unitary. The quantum walk is started to an initial node, and then the *qubit coin* is tossed, in order to choose in which direction it has to evolve.

Hence, a single step of the walk can be described by:

$$|\psi_{t+1}\rangle = \mathbf{SC}|\psi_t\rangle \tag{2.44}$$

9 An Hermitian matrix is a complex square matrix whose is equal to its conjugate transpose, formally: $A = A^\dagger$.

where $\mathbf{S}$ and $\mathbf{C}$ are two unitary operators describing the step and the coin toss. We can expand $|\psi_t\rangle$ as a superposition of basis states:

$$|\psi_t\rangle = \sum_{s,c} \alpha_{s,c}(t)|s,c\rangle \tag{2.45}$$

After T steps the state of the walk is defined by:

$$|\psi_T\rangle = (\mathbf{SC})^T|\psi_0\rangle \tag{2.46}$$

For a simple walk on an infinite line, the step operator $\mathbb{S}$ is defined by:

$$\mathbb{S}|s,c\rangle = |x+c,c\rangle \tag{2.47}$$

while $\mathbb{C}$, the operator describing the coin toss, in principle could be any unitary operator on the space of one qubit. It has been shown that all the proposed coins are equivalent up to a bias and take the form:

$$\mathbb{C} = \begin{pmatrix} \sqrt{\eta} & \sqrt{1-\eta} \\ \sqrt{1-\eta} & -\sqrt{\eta} \end{pmatrix} \tag{2.48}$$

where η is the probability of moving in positive direction, and $(1-\eta)$ the probability of moving in negative direction. If we set $\eta = 1/2$ (i.e.: unbiased coin) we obtain the so called *Hadamard operator*:

$$\mathbb{C}^{(H)} = \frac{1}{\sqrt{2}} \begin{pmatrix} 1 & 1 \\ 1 & -1 \end{pmatrix} \tag{2.49}$$

Setting $\eta = 0$ in Eq.(2.48) give oscillatory motion, while setting $\eta = 1$ gives an uniform motion. For higher dimension problem one has to choose the two unitary operators $\mathbf{S}$ and $\mathbf{C}$.

An example of quantum walk on a line have been presented by [Andrew M. Childs et al., 2002], while the full characterization of the probabilistic properties of discrete time quantum walk have been provided by [D. Aharonov et al., 2001].

Many results have been achieved thanks to the use of discrete time quantum walks: for example [Kempe, 2002] show that the hitting time of coined walks on a n-bit hypercube for one corner to the opposite is polynomial in n, while [Mackay et al., 2002] compared the classical and quantum spreading as a function of time. One can refer to [Kempe, 2003] for a review on coined quantum walks.

2.4.3 Continuous-Time Quantum Random Walks

The quantum analogue of the continuous-time random walk presented in Chapter 1 is the *continuous-time quantum walk*, and is defined as a dynamical process over the vertices of a graph $G = (V, E)$.

In the case of Continuous-Time Quantum Walks, the classical state vector is replaced by a vector of complex amplitudes over the vertices, such that their square norm sums to one. The lack of restriction on the phase and on the sign allows interference effects to take place.

The evolution of the walk is governed by the Schrödinger equation (Eq.(2.5)), which can be rewritten as:

$$\frac{\partial}{\partial t}|\psi_t\rangle = -i\mathcal{H}|\psi_t\rangle \tag{2.50}$$

where $\mathcal{H}$ denotes the time-independent Hamiltonian of the system. Given an initial state $|\psi_0\rangle$ we can solve Eq.(2.50) to find the state vector at time t:

$$|\psi_t\rangle = \mathrm{e}\,{-i\mathcal{H}t}|\psi_0\rangle \tag{2.51}$$

Usually, the Laplacian matrix is chosen as Hamiltonian for the system: indeed, it describes the case of a particle moving in empty space with zero potential energy. However it is possible to choose any other Hermitian operator encoding the structure of the graph as Hamiltonian for the system, such as the Adjacency matrix.

Again, we stress the fact that, since the evolution of the vector described by Equations (2.50) and (2.51) is governed by a complex unitary matrix, the evolution of the walk is non-ergodic and do not possess a limiting distribution. As a consequence, the evolution of the Classical Continuous Walk and the evolution of the Continuous-time Quantum Walk differs significantly.

Finally, one can note that (thanks to Thm. 1), we can write the Hamiltonian as $\mathcal{H} = \Phi\Lambda\Phi^\dagger$, where Λ denotes a diagonal matrix whose diagonal elements are the eigenvalues of the Hamiltonian, and Φ the corresponding eigenvectors. Hence we can rewrite Eq.(2.51) as:

$$|\psi_t\rangle = \Phi\,\mathrm{e}^{-i\Lambda t}\,\Phi^\dagger|\psi_0\rangle \tag{2.52}$$

Continuous time quantum walks have become an interesting field of research in the recent years: [Ahmadi et al., 2003] studied continuous time quantum walks in an N-cycle, [Moore and Russell, 2002] studied two continuous-time quantum walks on a n-dimensional hypercube, [Andrew M Childs et al., 2003] show an example of an algorithm based on continuous-time quantum walks in which it is possible to obtain an exponential speed-up with respect to the classical counterpart.

[Strauch, 2006] pointed out the relation between discrete-time quantum walks and continuous-time quantum walks on a infinite line.

In recent works, [Rossi, Torsello, Edwin R. Hancock, and Wilson, 2013], [Torsello, Gasparetto, et al., 2014] and [Rossi, Torsello, and Edwin R. Hancock, 2015] proposed a quantum algorithm to measure the similarity between a pair of unattributed graphs, based on the Quantum Jensen-Shannon Divergence ([Majtey et al., 2005]) through the evolution of continuous-time quantum walks on these graphs.

2.4.4 Decoherence

When designing an experiment one has to consider the lose of coherence due to interaction of the system with the surrounding environment, but this by itself does not make decoherence interesting. The important property of quantum decoherence that qualifies it as an interesting subject holds in the fact that it plays a fundamental

role in the transition from a Quantum system to a Classical one. Quantum walks are an example of systems in which decoherence can be studied and used to improve their algorithmic properties: instead of considering only pure quantum dynamics, we can include non-unitary operations, simulating the effect of Decoherence. Indeed, the crucial difference between classical walks and quantum walks stands is in the quantum coherence, i.e. the interferences due to the superposition of quantum states. Hence, a transition from quantum to classical has to "kill" those interferences. As seen in this Chapter, the easiest way to destroy the coherence is to perform a measurement: indeed if at each step we measure the position of the quantum walker (or the coin register, in the case of coined walks) on the graph, we obtain a classical walk.

A first idea, provided by [Kendon and Tregenna, 2003] and [Brun et al., 2003b], is to measure the position (or the coin) only with some probability p at each step: when $p = 0$ it corresponds to the quantum case, when $p = 1$ it corresponds to the classical one. Another option, provided by [Brun et al., 2003c] and [Brun et al., 2003a], is to achieve decoherence by defining a new coin at each iteration: doing so the coins do not interfere with themselves, thus obtaining the classical behaviour. [Alagic and Russell, 2005] studied a decoherence of coined random walks on an hypercube, observing that, for high decoherence rates, the Quantum Zeno effect[10] appears. [Fedichkin et al., 2006], instead, showed that decoherence can be useful in continuous time quantum walks on finite cycles.

For an excellent review on decoherent quantum walks, in which are formalized the concepts presented in this section, one can refer to [Kendon, 2007]. In Chapter 4, however, we will formalize the concept of Continuous-time quantum walk with decoherence.

10 The Quantum Zeno effect describes the inhibition, due to too frequent measurements, of the transition between quantum states, that causes the wave function to collapse. In particular, if the time between those measurements is short enough, the wave function collapses to its initial state. See [Itano et al., 1990] for more details.

3 STATE OF THE ART

As stated in Chapter 1, the definition of a structural signature is a crucial task in many application. Lot of work have been done in the years to provide structural node signatures to discriminate points in 2D images and, successively, in meshes representing 3D objects.

The first descriptors were based simply on the invariance of under global Euclidean transformation, trying to maximize shape similarities while aligning the objects: examples of these approaches are [Johnson and Hebert, 1999] and [Belongie et al., 2002]. Other approaches used *quaternions*[1] to transform the problem in a four-dimensional minimum eigenvalue problem (e.g.: [Faugeras and Hebert, 1983]), other approaches were based on least-square techniques (see for example [Lavallée and Szeliski, 1995]). All these approaches were designed to handle only rigid transformations.

Other less rigid approaches techniques were instead based on statistical-geometrical properties, comparing discrete histograms of geometric measures. The most influencing work that falls in this category is [Horn, 1984], while a recent one is [Tombari et al., 2010]. A variation of this concept was proposed by [Osada et al., 2001], in which they evaluated the Probability Distribution Function of a given measure (such as Euclidean distance) on two random points, measuring then the similarity of the resulting statistical signatures to compare different objects.

The Euclidean-transformation approaches were then extended focusing no more on Euclidean distance, but on the concept of geodesic distance[2], like for example the one proposed by [Elad and Kimmel, 2003], however such descriptors suffer from sensibility to topological and geometrical noise. Unfortunately, real application are strongly affected by such noises, so those descriptors result to be of poor use.

Thanks to the work of [Coifman and Lafon, 2006], the study of the so called *diffusion geometry* became popular: it focuses on the properties of the spectrum of the Laplace-Beltrami operator. The so called *diffusion distances* obtained by the Laplace-Beltrami operator, have been proved to be more robust compared to the previous approaches, and this encouraged to attempt to construct descriptors based on diffusion distance. Earlier contributions in this sense are represented for example by the *Global Point Signatures*, introduced by [Rustamov, 2007], and the *Shape DNA*, introduced by [Reuter et al., 2006].

1 Quaternions are an extension of the complex numbers with 3 imaginary bases i, j and k. They can be defined as a four dimensional vector space over the real numbers. Thus a quaternion is a number that takes the form $q = a + ix + jy + kz$. A quaternion has three operation: addition, scalar multiplication, and quaternion multiplication. For a detailed characterization of the properties of quaternions and their usage in Computer Vision one can refer to [Torsello, Rodolà, et al., 2011].

2 The geodesic distance between two nodes of a graph, is defined as the number of edges composing the shortest path among them. For more information on the distance, refer to [Bouttier et al., 2003].

The two more used and influencing results (the *Heat Kernel Signature* and the *Wave Kernel Signature*) are themselves related to the analysis of the spectrum of the Laplace-Beltrami operator, and will be presented in this chapter.

Other approaches are instead based on machine learning, for example [A. M. Bronstein, 2011] and [Litman and A. M. Bronstein, 2014].

The feature descriptors that is going to be introduced by this thesis is related to the spectrum of the Laplace-Beltrami Operator, and provide a Quantum Mechanical approach based of building a Decoherent Quantum Random Walk on the graph.

3.1 THE HEAT KERNEL SIGNATURE

The Heat Kernel Signature, introduced by [Sun et al., 2009], is a node signature defined by restricting the heat kernel (which is associated with the Laplace-Beltrami operator) to the temporal domain.

The heat equation can be written as:

$$\frac{\partial}{\partial t}u(x,t) = \Delta u(x,t) \tag{3.1}$$

where Δ is the Laplace-Beltrami operator and $u(x,t)$ indicates the diffusion of heat at time t at point x. Assuming some initial (time $t = 0$) heat distribution $u_0(t)$, we can apply to the initial distribution the heat operator:

$$u(t,x) = \int h_t(x,y)u_0(t)\mathrm{d}y \tag{3.2}$$

The minimum function $h_t(x,y)$ that satisfies Eq.(3.2) is called the *heat kernel* and corresponds to the amount of heat transferring from x to y after a time t is passed giving a unit heat source at x. We can also see the heat kernel as the transition probability density from x to y by a random walk of length t.

We can express the *heat kernel* as follows:

$$h_t(x,y) = \sum_{k\geq 1} \mathrm{e}^{-\lambda_k t}\,\phi_k(x)\phi_k(y) \tag{3.3}$$

where λ_i and ϕ_i are respectively the i-th eigenvalue and the i-th eigenvector of the Laplace-Beltrami operator. We can see the heat kernel as a low-pass filter and interpret $\exp(-\lambda_k t)$ as the frequency response of the heat kernel: the bigger is the time parameter t, the lower is the cut-off frequency of the filter and consequently the bigger is the support of h_t.

The *Auto Diffusion Function* [Gebal et al., 2009], defined as:

$$h_t(x,x) = \sum_{k\geq 1} \mathrm{e}^{-\lambda_k t}\,\phi_k(x)^2 \tag{3.4}$$

instead represents the quantity of heat that after a time t remains at x.

The heat kernel provides a characterization of the neighbourhood of a given point x, however it would be hard to get for each point x a signature defined by the family

of functions parametrized on time $\{h_t(x,\cdot)\}_{t>0}$, so [Sun et al., 2009] defined the Heat Kernel Signature for a point x as a vector whose components are the values of the Auto Diffusion Function sampled at a finite set of times $t_1,\dots,t_n$:

$$\mathrm{HKS}(x) = \begin{pmatrix} h_{t_1}(x,x) \\ \vdots \\ h_{t_n}(x,x) \end{pmatrix} \tag{3.5}$$

The resulting multi-scale invariant descriptor is stable under perturbations and can be estimated efficiently, as it is concise but still informative. Finally, [Gebal et al., 2009] defined the distance between two Heat Kernel signatures of two points x and x' on a Manifold Ω at the scale specified by the time interval $[t_1,t_2]$ as:

$$d_{[t_1,t_2]}(x,x') = \left(\int_{t_1}^{t_2} \left(\frac{|h_t(x,x) - h_t(x',x')|}{\int_\Omega h_t(x,x)\mathrm{d}x} \right)^2 \mathrm{d}\log(t) \right)^{\frac{1}{2}} \tag{3.6}$$

In practice, this distance is computed by sampling the Heat Kernel Signature uniformly over the logarithmic scaled temporal domain obtaining two vectors representing the signatures for the two points, then the integral in Eq.(3.6) is estimated by computing the ℓ^2-norm[3] of the difference between the two vectors.

As [Aubry et al., 2011] and [A. M. Bronstein, 2011] pointed out, being the Heat Kernel Signature a collection of low-pass filters, it is dominated by low frequencies and so it describes well only informations about the global structure, damaging the ability of the descriptor of precisely localize features. In particular, the distance from the kernel computed on a point x to his neighbourhood increases slowly, and this results in bad localization. Finally, the time parameter plays a central role, but has no straightforward interpretation in the point of view of the shape, and then the choice of the set of times has to be done heuristically.

A scale-invariant version of this kernel has be introduced by [M. M. Bronstein and Kokkinos, 2010].

3 The ℓ^n-norm for a vector $\mathbf{x}$ of length m is defined as:

$$\|\mathbf{x}\|_n = \sqrt[n]{\sum_{k=1}^{m} |x_k|^n}$$

In particular, the ℓ^2-norm is defined as:

$$\|\mathbf{x}\|_2 = \|\mathbf{x}\| = \sqrt{\sum_{k=1}^{n} |x_k|^2}$$

and it also called the Euclidean norm. The term Euclidean norm may cause confusion as it is also used to indicate the Frobenius norm, which is a matrix norm and is defined as:

$$\|A\|_F = \sqrt{\sum_{i=1}^{m}\sum_{j=1}^{n} |a_{ij}|^2} = \sqrt{\mathrm{tr}(A^\dagger A)}$$

3.2 THE WAVE KERNEL SIGNATURE

The Wave Kernel Signature, introduced by [Aubry et al., 2011], is a spectral descriptor derived from the Laplace Beltrami Operator used for characterizing points on non-rigid three-dimensional shapes and represents the probability of a quantum particle with a certain energy distribution to be located at a specific location. This approach remedies to the problem of the Heat Kernel Signature related to its poor feature localization reducing the influence of low frequencies and allowing better separation of frequencies band scale, as it can be view as a band-pass filter.

The evolution of a quantum particle x on a surface is governed by its wave function $\psi(x,t)$, which is a solution of the Schrödinger equation described in Eq.(2.5):

$$\frac{\partial}{\partial t}\psi(x,t) = i\Delta\psi(x,t) \tag{3.7}$$

where Δ is the Laplace-Beltrami operator.

Note that, even if Eq.(3.7) looks similar to Eq.(3.1), ψ represents no more the diffusion and has an oscillatory behaviour due to the multiplication of the complex unit by Δ.

Assume that a quantum particle, whose position is unknown, at time $t = 0$ has a energy distribution $f(e) = f(\lambda)$[4]. Then we can express the wave function as:

$$\psi_E(x,t) = \sum_0^\infty \mathrm{e}^{i\lambda_k t}\,\phi_k(x) f_E(\lambda_k) \tag{3.8}$$

Then, the probability to measure at time t the particle at point x is given by $|\psi_E(x,t)|^2$. The Wave Kernel signature of a point x given an energy probability distribution f_E^2 is defined as:

$$\begin{aligned} \mathrm{WKS}(E,x) &= \lim_{T\to\infty}\frac{1}{T}\int_0^T |\psi_E(x,t)|^2 \\ &= \sum_{k=0}^{\infty} \phi_k(x)^2 f_E(\lambda_k)^2 \end{aligned} \tag{3.9}$$

Note that, integrating over time, the time parameter has been replaced by energy that we expressed by the eigenvalues of the Laplace-Beltrami operator: this gives a natural notion of scale, as was shown in Section 1.4.2.

We now need to define an appropriate energy function f_E^2. In the original paper [Aubry et al., 2011], after a perturbation analysis of the Laplacian spectrum, considered a family of log-normal distributed random variables:

$$f_e(\lambda) \propto \exp\left(-\frac{(\log(e)-\log(\lambda))^2}{\sigma^2}\right) \tag{3.10}$$

Once we have fixed this family of energy distributions, we can define the *Wave Kernel Signature* for the point x as the vector of the probabilities $p_e(x)$ to measuring

4 Energy is strongly related with frequency, so we use $f(\lambda)$ in place of $f(e)$, where λ are the eigenvalues of the Laplace-Beltrami operator.

a quantum particle with an initial energy distribution sampled in the logarithmic scale $f_e(\lambda)$ at x:

$$\mathrm{WKS}(x, e) = \begin{pmatrix} p_{e_1}(x) \\ \vdots \\ p_{e_n}(x) \end{pmatrix} \tag{3.11}$$

To compare two Wave Kernel signatures for two different points x and x', is defined a distance based on the ℓ^1-norm of the normalized signature difference:

$$d(x, x') = \int_{e_{\min}}^{e_{\max}} \left| \frac{\mathrm{WKS}(x, e) - \mathrm{WKS}(x', e)}{\mathrm{WKS}(x, e) + \mathrm{WKS}(x', e)} \right| \mathrm{d}e \tag{3.12}$$

This signature is considered the state of the art in the field of structural node signatures.

4 DECOHERENT WALK SIGNATURE

Similartly to the Schrödinger equation, the Liouville-Von Neumann equation describes how a density operator evolves in time:

$$\frac{\mathrm{d}\rho(t)}{\mathrm{d}t} = -i[H, \rho(t)] \tag{4.1}$$

where H is a time independent Hamiltonian for the system, $[a, b] \equiv ab - ba$, is the commutator and $\rho(t) = |\psi_t\rangle\langle\psi_t|$ is the density operator associated with the continuous-time quantum walk at time t, which in the case of a mixed state takes the form $\sum_t p_t|\psi_t\rangle\langle\psi_t|$.
We let the Hamiltonian H be the graph Laplacian (Eq.(1.4)).

Let $\mathcal{L}$ be the Liouville super-operator which acts on ρ, than the previous equation can be rewritten in terms of $\mathcal{L}$ as:

$$\frac{\mathrm{d}}{\mathrm{d}t}\rho(t) = \mathcal{L}\rho(t) \tag{4.2}$$

We can compute the density matrix at time t starting from a initial density matrix $\rho(0)$ as follows:

$$\rho(t) = \mathrm{e}^{\mathcal{L}t}\,\rho(0) \tag{4.3}$$

As shown in Chapter 2, in quantum mechanics decoherence is the irreversible process that describes the emergency of classical properties on the quantum system, due to the interaction with the surrounding environment. In other words, it describes the transition of quantum density matrices to classical probability distributions. It is usually modelled as a non-unitary evolution of the quantum walk.

We can simulate the effects of decoherence by reducing some or all of the off-diagonal elements of ρ. Formally, we can rewrite Eq.(4.1) as:

$$\frac{\mathrm{d}\rho(t)}{\mathrm{d}t} = -i[L, \rho] - p\rho + p\mathcal{P}\rho \tag{4.4}$$

where p is the is the rate with which we add decoherence in the walk and $\mathcal{P}$ is an operator which represents the effect of noise on ρ.

A solution of Eq.(4.4) can be found by rewriting it in terms of the Liouville super-operator $\mathcal{L} = (-i\mathbb{A} + p\mathbb{B})$, which yields:

$$\begin{aligned}\frac{\mathrm{d}}{\mathrm{d}t}\,\mathrm{vec}(\rho(t)) &= \mathcal{L}\,\mathrm{vec}(\rho(t)) \\ &= (-i\mathbb{A} + p\mathbb{B})\,\mathrm{vec}(\rho(t))\end{aligned} \tag{4.5}$$

Where $\mathbb{A} = I \otimes L - L \otimes I$[1] and $\mathbb{B}$ is a diagonal matrix having $\mathbb{B}_{xx} = 0$ if $\text{vec}(\rho(x))$ corresponds to a diagonal element of ρ, formally:

$$\mathbb{B} = \sum_i p_i^\dagger \otimes p_i - I \tag{4.6}$$

Having defined the superoperator and the two composing matrices $\mathbb{A}$ and $\mathbb{B}$, we can rewrite Eq.(4.3) as follows:

$$\text{vec}(\rho(t)) = \mathrm{e}^{\mathcal{L}t}\,\text{vec}(\rho(0)) = \mathrm{e}^{(-i\mathbb{A}+p\mathbb{B})t}\,\text{vec}(\rho(0)) \tag{4.7}$$

4.1 THE SIGNATURE

In our setting, rather than determining the density matrix at a specific time t, we are interested in studying how decoherence rate influences the dynamic of the system on different energy levels.

We started defining the initial density matrix in a way that it depends to an energy level, formally:

$$\rho(E, 0) = \Psi_E(0)\Psi_E(0)^\dagger \tag{4.8}$$

where:

$$\begin{aligned}\Psi_E(0) &= \sum_\lambda \mathrm{e}^{i\lambda t}\,\phi_\lambda f_E(\lambda) \\ &= \sum_\lambda \phi_\lambda f_E(\lambda) \\ &= \phi^\dagger f_E\end{aligned} \tag{4.9}$$

As [Aubry et al., 2011] did in their approach, we defined the energy function f_E in the logarithmic energy scale as follows:

$$\begin{aligned}f_E^2(x) &= \frac{1}{x\sqrt{2\pi\sigma^2}} \exp\left(-\frac{(\log(x) - \log(E))^2}{2\sigma^2}\right) \\ f_E(x) &= \frac{1}{\sqrt[4]{x^2 2\pi\sigma^2}} \exp\left(-\frac{(\log(x) - \log(E))^2}{4\sigma^2}\right)\end{aligned} \tag{4.10}$$

1 The symbol $\otimes$ here denotes the Kronecker product. It is a generalization of the outer product between vectors and matrices and results in the matrix of the tensor product with respect to a standard choice of basis. Suppose to have to matrices A and B, of sizes respectively $m \times n$ and $p \times q$, then $A \otimes B$ gives a $mp \times nq$ matrix:

$$A \otimes B = \underbrace{\left.\begin{bmatrix} a_{11}B & a_{12}B & \dots & a_{1n}B \\ a_{21}B & a_{22}B & \dots & a_{2n}B \\ \vdots & \vdots & \vdots & \vdots \\ a_{m1}B & a_{m2}B & \dots & a_{mn}B \end{bmatrix}\right\}_{mp}}_{nq}$$

We did not considered the multiplicative term, hence we chosen the following family of energy functions:

$$f_E(\lambda) \propto \exp\left(-\frac{(\log(E)-\log(\lambda))^2}{4\sigma^2}\right) \tag{4.11}$$

Note that this is not the only possible choice of f_E, we decided to use this function to stay as close as possible to the approach provided by the Wave Kernel Signature. Hence Eq.(4.9) become:

$$\Psi_E(0) = \sum_k \phi_k \exp\left(-\frac{(\log(E)-\log(\lambda_k))^2}{4\sigma^2}\right) \tag{4.12}$$

where λ and ϕ are respectively the eigenvalues and the eigenvectors of the Laplacian. Now it is possible to rewrite the initial density matrix which depends on the energy level E in Eq.(4.8) as follows:

$$\begin{aligned}\rho(E,0) &= \Psi_E(0)\Psi_E^\dagger(0) \\ &= \sum_{n,k} \phi_n \phi_k^\dagger \exp\left(-\frac{(\log(E)-\log(\lambda_h))^2 + (\log(E)-\log(\lambda_k))^2}{4\sigma^2}\right)\end{aligned} \tag{4.13}$$

We are interested in integrating the walk, rather than in computing the density matrix at a specific time. In particular we want to compute:

$$\mathrm{vec}(\rho(E,t)) = \frac{1}{T}\int_1^T \mathrm{vec}(\rho(E,t))\mathrm{d}t \tag{4.14}$$

In order to compute the exponentiation of Eq.(4.7), we need the spectral decomposition of the Liouville superoperator. By construction it is not Hermitian, since both $\mathbb{A}$ and $\mathbb{B}$ are symmetric, so we get:

$$\begin{aligned}\mathrm{vec}(\rho(E,t)) &= \mathrm{e}^{\mathcal{L}t}\,\mathrm{vec}(\rho(E,0)) \\ &= S\,\mathrm{e}^{Dt}\,S^{-1}\,\mathrm{vec}(\rho(E,0))\end{aligned} \tag{4.15}$$

where D and S are respectively the eigenvalues and the corresponding eigenvectors of the Liouville superoperator $\mathcal{L} = -i\mathbb{A} + p\mathbb{B}$.

Hence Eq.(4.14) became:

$$\begin{aligned}\mathrm{vec}(\rho(E,t)) &= \frac{1}{T}\int_1^T \mathrm{vec}(\rho(E,t))\mathrm{d}t \\ &= \frac{1}{T}\int_1^T \mathrm{e}^{\mathcal{L}t}\,\mathrm{vec}(\rho(E,0))\mathrm{d}t \\ &= \frac{1}{T}\left[S\,\mathrm{e}^{Dt}\,S^{-1}\right]_0^T \mathrm{vec}(\rho(E,0)) \\ &= \frac{1}{T}S\left[\mathrm{e}^{Dt}\right]_0^T S^{-1}\,\mathrm{vec}(\rho(E,0)) \\ &= \frac{1}{T}SD^{-1}\left(\mathrm{e}^{DT} - \mathbb{1}\right)S^{-1}\,\mathrm{vec}(\rho(E,0))\end{aligned} \tag{4.16}$$

where D^{-1} and $\exp(DT)$ are diagonal matrices, and $\mathbb{1}$ is the identity matrix.

The diagonal element of $\rho(E,t) = [\mathrm{vec}(\rho(E,t))]_{(n,n)}$[2] corresponds to the probabilities of the particle to be measured in the corresponding node after the time t. Hence we defined the signature of a node x in the energy levels E for fixed decoherence rate p as follows:

$$DWS_{E,p}(x) = \mathrm{diag}\left(\left[\frac{1}{T}SD^{-1}\left(\mathrm{e}^{DT} - \mathbb{1}\right)S^{-1}\,\mathrm{vec}(\rho(E,0))\right]_{(n,n)}\right) \tag{4.17}$$

The resulting signature can be viewed as a three-dimensional matrix, and to compare the signatures of two nodes x and x' one can compute the ℓ^2-norm of the vectorization of the corresponding signatures:

$$d(x,x') = \sqrt{|\,\mathrm{vec}(DWS_{\mathbf{E},\mathbf{p}}(x)) - \mathrm{vec}(DWS_{\mathbf{E},\mathbf{p}}(x'))|^2} \tag{4.18}$$

where $\mathbf{E}$ and $\mathbf{p}$ represents the vectors of the energy levels and of the decoherence rates.

2 The notation $[x]_{(n,n)}$ indicates the matricization of the array x of size n^2 into an n-by-n matrix, formally:

$$[x]_{(n,n)} = [(x_1,\ldots,x_n,\ldots,x_{n^2-n+1},\ldots,x_{n^2})]_{(n,n)} = \underbrace{\left.\begin{bmatrix} x_1 & \cdots & x_n \\ \vdots & \vdots & \vdots \\ x_{n^2-n+1} & \cdots & x_{n^2} \end{bmatrix}\right\}_{n}}_{n}$$

5 TEST RESULTS

In this chapter will be presented the results of the tests performed on the signature presented in Chapter 4. All the tests have been performed on a Toshiba Satellite L50-A-170[1] running Ubuntu 14.10 64bits. The signatures and the tests that we are going to introduce have been implemented in Matlab (ver. R2013a)[2].

In the case of the WKS and of the HKS, we used the default parameters provided with the original code.

For the test presented in the following, we simulated the effect of decoherence treating it as an uniform noise on the off-diagonal elements of the density matrix. Note that this is the most simple case, different approaches are possible. We also recall that the energy function that we choose in Eq.(4.11) is not the only possible one.

We will start studying the behaviour of our signature when applied in a 6×6 graph, that is represented in Figure 5.1.

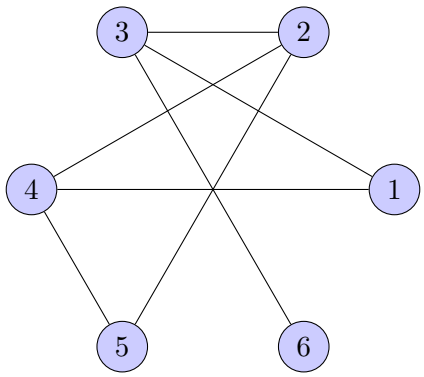

Figure 5.1: A simple 6×6 connected graph.

Take as example the graph presented in Figure 5.1. For this test we set $T = 1000$ (see Eq.(4.17)) and we let the decoherence rate vary from 0 to 0.2, with a step of 0.01. The other parameters (the energy levels and the standard deviation of the log-normal distribution) are computed in the same way that [Aubry et al., 2011] did for their approach.

The signatures of each node of the graph in Figure 5.1 are presented in Table 5.1.

1 Hardware details can be find on http://goo.gl/WynJwS.

2 The Matlab code of the Heat Kernel Signature can be downloaded on http://goo.gl/F4WmOI, while the code for the Wave Kernel Signature can be downloaded on http://goo.gl/tlpR4i.

Node	Scaled HKS	WKS	DKS
1	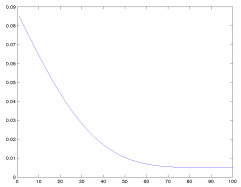	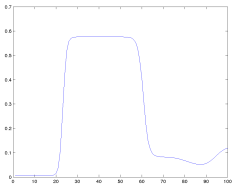	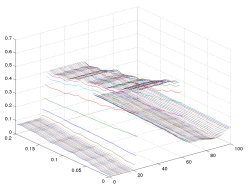
2	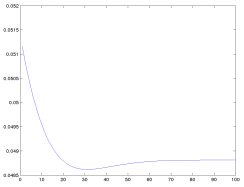	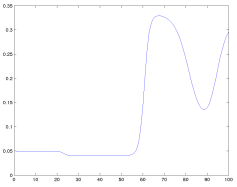	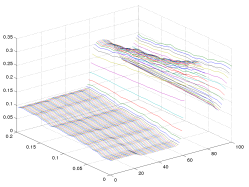
3	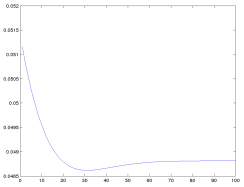	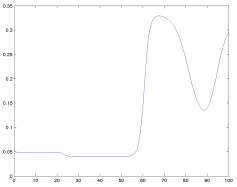	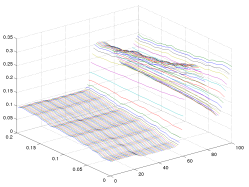
4	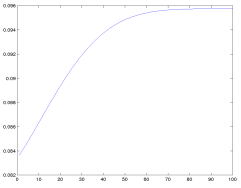	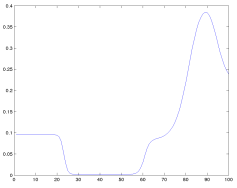	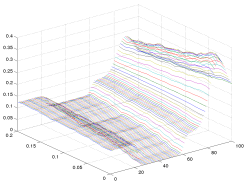
5	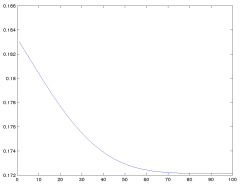	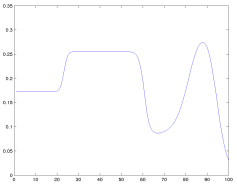	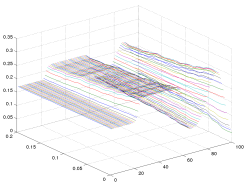
6	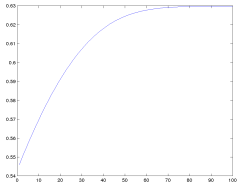	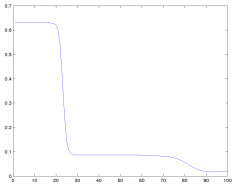	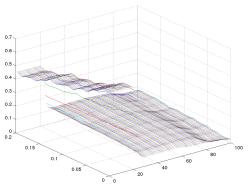

Table 5.1: Graphical representation of the signatures of a simple 6×6 graph. For the WKS, on the x axis there is the time, while on the y axis there is the response of the signature, for the HKS and for the DKS on the x axis there is the energy level, the probability is on the y axis for the WKS and in the z axis for the DWS, while in the y axis of the DWS there is the decoherence rate.

5.1 DECOHERENCE EFFECT

We can graphically show the effect of decoherence in probabilities of quantum particles to be located in the nodes of the graph in Figure 5.1. In particular, we computed

such a probability varying the time from 0 to 20, at two different energy levels and at three different rates of energies, that is at rate 0 (no decoherence), at rate 0.1 and at rate 0.2.

The resulting plot is presented in Table 5.2.

Rate	E_1	E_2
0	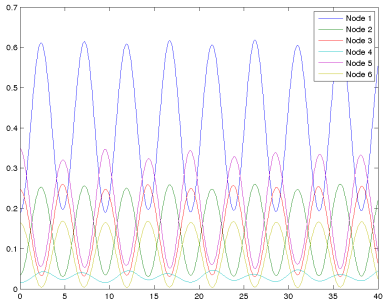	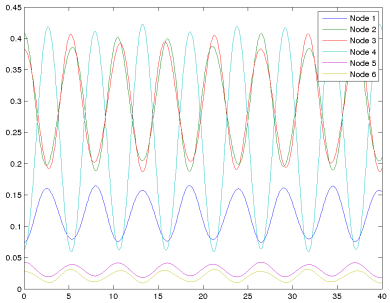
0.1	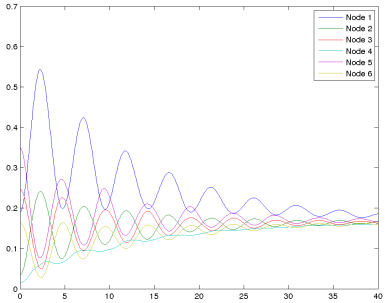	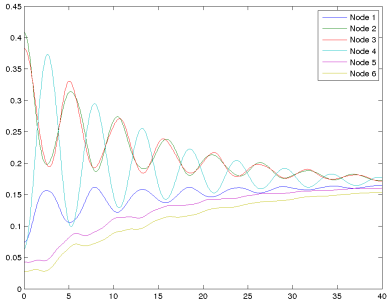
0.2	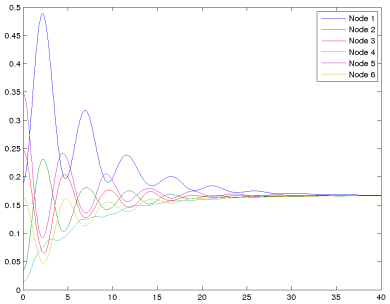	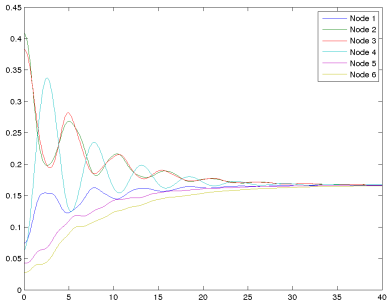

Table 5.2: Effects of decoherence: the probability for a quantum particle to be in the nodes of the graph giving three level of decoherence (no decoherence, 0.1 decoherence and 0.2 decoherence) on times varying from 0 to 40. The probabilities are computed on two different energy levels E_1 and E_2.

We can see that when there is no decoherence the probabilities have an oscillatory behaviour, that when we add decoherence is suppressed more and more in time, untill the probabilities converges to the uniform distribution, which indeed is the limit of the classical walk.

5.2 ROBUSTNESS

The first test that we performed was to generate some connected random graphs of different density (but not too dense or too sparse) of sizes 10, 15, 20 and 25, and test how their signatures are robust to edge insertion or deletion.

In particular, for each signature:

- We generated 25 random graphs of size 10, adding or deleting random from 1 to 10 random edges (this test was repeated 10 times for each graph).
- We generated 25 random graphs of size 15, adding or deleting random from 1 to 15 random edges (this test was repeated 15 times for each graph).
- We generated 20 random graphs of size 20, adding or deleting random from 1 to 20 random edges (this test was repeated 20 times for each graph).
- We generated 20 random graphs of size 25, adding or deleting random from 1 to 20 random edges (this test was repeated 20 times for each graph).

We present the results of those tests in Table 5.3.

From Table 5.3 we can say that our signature is at least as robust as the Wave Kernel Signature on perturbations on the graph such as edge insertion or edge deletion.

5.3 EXPERIMENTS ON REAL WORLD EXAMPLES

We finally tested our algorithms on two standard database of graphs: The Shock dataset ([Torsello and Edwin R Hancock, 2006]) and the MUTAG dataset([Debnath et al., 1991]) . In particular:

Shock dataset It is composed by graphs from a database of 2D shapes. Each graph is a medial axis-based representation of the differential structure of the boundary of the 2D shape. It is composed by 150 graph, divided in 10 classes each composed by 15 graphs. The bigger graph is composed by 33 vertices, while the smaller one is composed by 4 vertices. The average number of vertices for the graphs is 13.

MUTAG dataset It is a dataset representing 188 mutagenic aromatic and heteroaromatic compunds labeled in two classes according to whether or not they have a magnetic effect on the bacterium *Salmonella Typhimurium*. The bigger graph is composed by 28 vertices,while the smaller one has 10 vertices. The average number of vertices for the graphs is 18.

In the following we present the results of our tests. Note that there was no correspondence between nodes in the graphs composing the dataset, hence we needed to use the Hungarian algorithm ([Kuhn, 2010]) in order to find the best match among nodes given the resulting signature, in order to minimize the total distance between the signatures.

n	**Scaled HKS**	**WKS**	**DWS**
10	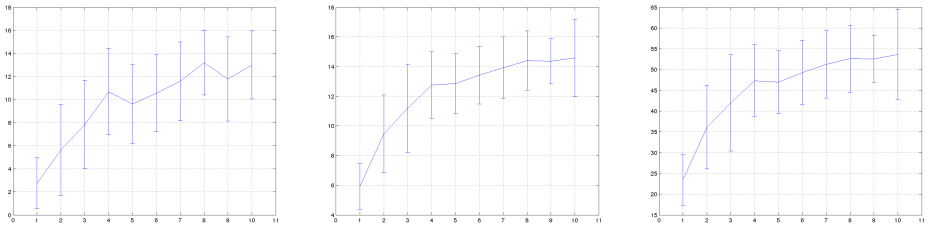		
15	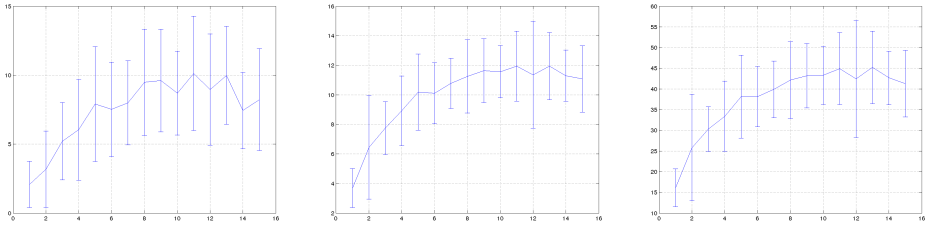		
20	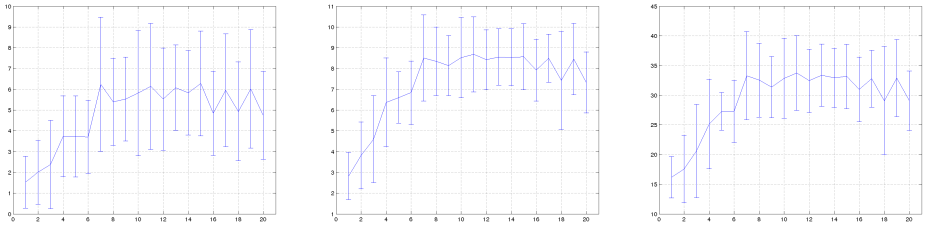		
25	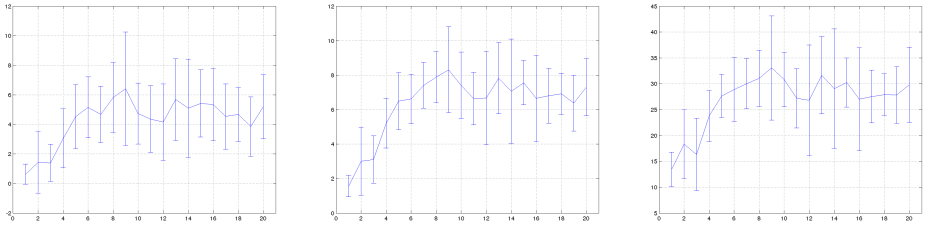		

Table 5.3: Robustness of the signatures.

5.3.1 Shock dataset

The results of the tests on the Shock graph dataset are presented in Table 5.4, where we graphically show the distances between measured signatures. The darker is the cell the more similar are the measured signatures. Note that this dataset is very complicated to classify.

The results, for all the signatures, are not so good. But, as we stated, this is hard to distinguish among different classes of this dataset.

5.3.2 MUTAG dataset

The results of the tests on the MUTAG dataset are presented in Table 5.5, where we graphically show the distances between measured signatures. The darker is the cell the more similar are the measured signatures.

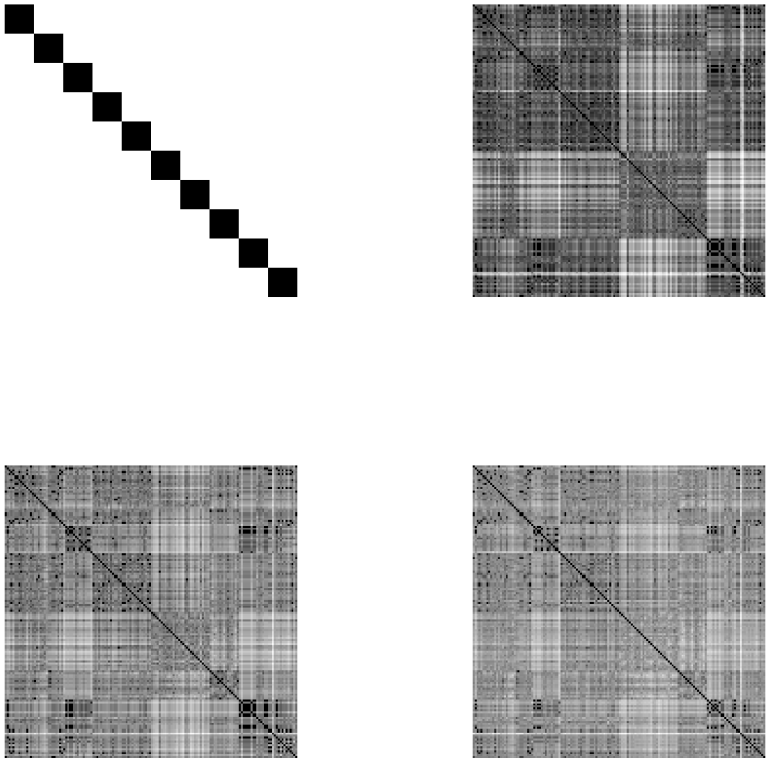

Table 5.4: Similarities between the signatures of the graphs composing the Shock dataset. The darker is the cell, the higher is the similarity between the two signatures. The first picture indicates the classes, the second picture indicates the results for the scaled heat signature, the third picture indicates the results for the Wave Kernel Signature and the last picture indicates the results for our signature.

Note that in this case the Wave Kernel Signature and our signature found better the similarities among the classes. The Heat Kernel signature, on the other hand, provide a poor discrimination of the graphs.

Looking at the presented results we can say that our signature behaves better than the Heat Kernel Signature, while it behaves very similar to the Wave Kernel Singature. We stress out that this is due to the fact that, in this initial set-up, the signature is build to extend the WKS, but still remains similar to it, as the initial density matrix is strongly related to the Wave Kernel Signature and the decoherence is added in an uniform way.

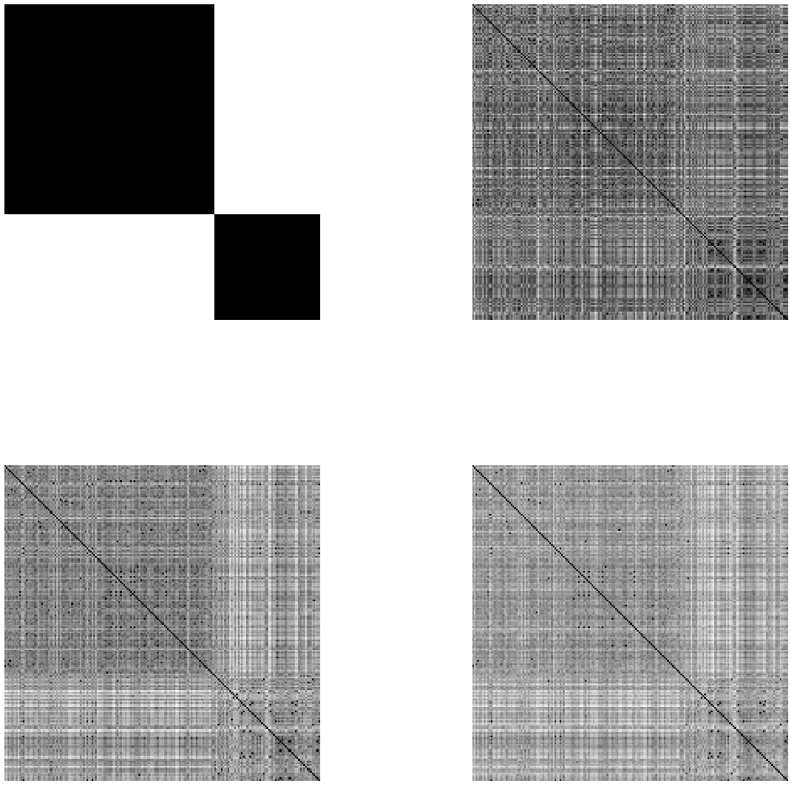

Table 5.5: Similarities between the signatures of the graphs composing the MUTAG dataset. The darker is the cell, the higher is the similarity between the two signatures. The first picture indicates the classes, the second picture indicates the results for the scaled heat signature, the third picture indicates the results for the Wave Kernel Signature and the last picture indicates the results for our signature.

6 CONCLUSIONS

In this work we provided an overview to Quantum Computation, focusing on the main concepts that we have used to provide our signature: the Decoherent Walk Signature, a graph node feature descriptor based on a continuous-time random walk with decoherence.

Our approach merges the wave-like transport of quantum walks, and in particular of the Wave Kernel Signature, with the diffusion process of classical walks, and in particular the Heat Kernel Signature.

Tests on both synthetic and real world graphs, have exhibit strong advantages over the Heat Kernel Signature and marginal ones with respect to the Wave Kernel Signature.

6.1 FUTURE WORKS

In order to improve our signature, first of all we need to decrease its computational complexity. Indeed, computing the eigenvalues and the eigenvectors of the Liouville superoperator in Eq.(4.16) become infeasible even with graphs of small size (greater than 50 nodes), since this operation is cubic with respect to a matrix that has a size that is quadratic with respect to the original problem. Once this problem will be fixed, it will be possible to deal with big graphs and to test our approach on meshes representing 3D objects.

The idea to solve this problem is to perform a perturbation analysis of the eigenvalues and eigenvectors of the components of the superoperator, noting that the "main" component of the superoperator is a matrix whose eigenvalues are known, since it is created starting from the Laplace-Beltrami operator.

Moreover, as we already stated, the parameters in Eq.(4.11) (as well as the function itself) where fixed according to the one used as default in the Wave Kernel Signature. It will be interesting to test the behaviour of the signature with other parameters and, most importantly, with other energy functions. Another test that can be useful is to use as initial Hamiltonian in place of the Laplacian another operator describing the state of the graph, such as the adjacency matrix.

Finally, as we stated in Chapter 4, in this initial setting we defined the decoherence as an operator that uniformly add the same rate of decoherence on the off-diagonal elements of the initial density matrix. It would be interesting to set up different approaches. Decoherence rates and time in which to integrate the dynamics are other parameters that need further investigation.

BIBLIOGRAPHY

Aharonov, Dorit, Andris Ambainis, Julia Kempe, and Umesh Vazirani

2001 "Quantum Walks on Graphs", in *Proceedings of the Thirty-third Annual ACM Symposium on Theory of Computing*, STOC '01, ACM, Hersonissos, Greece, pp. 50-59, ISBN: 1-58113-349-9, DOI: 10.1145/380752.380758, http://doi.acm.org/10.1145/380752.380758.

Aharonov, Yakir, Luiz Davidovich, and Nicim Zagury

1993 "Quantum random walks", *Phys. Rev. A*, 48 (2 Aug. 1993), pp. 1687-1690, DOI: 10.1103/PhysRevA.48.1687, http://link.aps.org/doi/10.1103/PhysRevA.48.1687.

Ahmadi, Amir, Ryan Belk, Christino Tamon, and Carolyn Wendler

2003 "On Mixing in Continuous-time Quantum Walks on Some Circulant Graphs", *Quantum Info. Comput.*, 3, 6 (Nov. 2003), pp. 611-618, ISSN: 1533-7146, http://dl.acm.org/citation.cfm?id=2011556.2011560.

Alagic, Gorjan and Alexander Russell

2005 "Decoherence in Quantum Walks on the Hypercube", *Physical Review A*, 72, 6 (Dec. 2005), p. 062304, DOI: 10.1103/PhysRevA.72.062304, http://dx.doi.org/10.1103/PhysRevA.72.062304.

Aubry, Mathieu, Ulrich Schlickewei, and Daniel Cremers

2011 "The Wave Kernel Signature: A Quantum Mechanical Approach to Shape Analysis.", in *ICCV Workshops*, IEEE, pp. 1626-1633, ISBN: 978-1-4673-0062-9, http://dblp.uni-trier.de/db/conf/iccvw/iccvw2011.html#AubrySC11.

Auletta, Gennaro, Mauro Fortunato, and Giorgio Parisi

2009 *Quantum Mechanics*, Cambridge University Press, ISBN: 9781139478458, http://books.google.it/books?id=f9L8PuDK5BgC.

Belongie, S., J. Malik, and J. Puzicha

2002 "Shape matching and object recognition using shape contexts", *Pattern Analysis and Machine Intelligence, IEEE Transactions on*, 24, 4 (Apr. 2002), pp. 509-522, ISSN: 0162-8828, DOI: 10.1109/34.993558.

Biasotti, Silvia, Simone Marini, Michela Mortara, Giuseppe Patanè, Michela Spagnuolo, and Bianca Falcidieno

2003 "3D shape matching through topological structures", in *Discrete Geometry for Computer Imagery*, Springer, pp. 194-203.

Bouttier, J., P. Di Francesco, and E. Guitter

2003 "Geodesic distance in planar graphs", *Nuclear Physics B*, 663, 3, pp. 535-567, ISSN: 0550-3213, DOI: http://dx.doi.org/10.1016/S0550-3213(03)00355-9, http://www.sciencedirect.com/science/article/pii/S0550321303003559.

Bronstein, Alexander M.

2011 "Spectral descriptors for deformable shapes", *CoRR*, abs/1110.5015, http://arxiv.org/abs/1110.5015.

Bronstein, Michael M. and Iasonas Kokkinos

2010 "Scale-invariant heat kernel signatures for non-rigid shape recognition.", in *CVPR*, IEEE, pp. 1704-1711, http://dblp.uni-trier.de/db/conf/cvpr/cvpr2010.html#BronsteinK10.

Brun, Todd A., Hilary A. Carteret, and Andris Ambainis

2003a "Quantum random walks with decoherent coins", *Physical Review A*, 67, 3, 032304 (Mar. 2003), p. 032304, DOI: 10.1103/PhysRevA.67.032304, eprint: quant-ph/0210180.

2003b "Quantum to Classical Transition for Random Walks", *Physical Review Letters*, 91, 13, 130602 (Sept. 2003), p. 130602, DOI: 10.1103/PhysRevLett.91.130602, eprint: quant-ph/0208195.

2003c "Quantum walks driven by many coins", *Physical Review A*, 67, 5, 052317 (May 2003), p. 052317, DOI: 10.1103/PhysRevA.67.052317, eprint: quant-ph/0210161.

Childs, Andrew M, Richard Cleve, Enrico Deotto, Edward Farhi, Sam Gutmann, and Daniel A Spielman

2003 "Exponential algorithmic speedup by a quantum walk", in *Proceedings of the thirty-fifth annual ACM symposium on Theory of computing*, ACM, pp. 59-68, eprint: quant-ph/0209131.

Childs, Andrew M., Edward Farhi, and Sam Gutmann

2002 "An Example of the Difference Between Quantum and Classical Random Walks", *Quantum Information Processing*, 1, 1/2 (Apr. 2002), pp. 35-43, ISSN: 1570-0755, DOI: 10.1023/A:1019609420309, http://dx.doi.org/10.1023/A:1019609420309.

Chung, Fan R.K.

1997 *Spectral graph theory*, American Mathematical Soc., vol. 92.

Coifman, Ronald R. and Stéphane Lafon

2006 "Diffusion maps", *Applied and Computational Harmonic Analysis*, 21, 1, Special Issue: Diffusion Maps and Wavelets, pp. 5-30, ISSN: 1063-5203, DOI: http://dx.doi.org/10.1016/j.acha.2006.04.006, http://www.sciencedirect.com/science/article/pii/S1063520306000546.

Debnath, Asim Kumar, Rosa L. Lopez de Compadre, Gargi Debnath, Alan J. Shusterman, and Corwin Hansch

1991 "Structure-activity relationship of mutagenic aromatic and heteroaromatic nitro compounds. Correlation with molecular orbital energies and hydrophobicity", *Journal of Medicinal Chemistry*, 34, 2, pp. 786-797, DOI: 10.1021/jm00106a046, eprint: http://dx.doi.org/10.1021/jm00106a046.

Elad, A. and R. Kimmel

2003 "On Bending Invariant Signatures for Surfaces", *IEEE Trans. Pattern Anal. Mach. Intell.*, 25, 10 (Oct. 2003), pp. 1285-1295, ISSN: 0162-8828, DOI: 10.1109/TPAMI.2003.1233902, http://dx.doi.org/10.1109/TPAMI.2003.1233902.

Farhi, Edward and Sam Gutmann

1998 "Quantum computation and decision trees", *Physical Review A*, 58 (Aug. 1998), pp. 915-928, DOI: 10.1103/PhysRevA.58.915, eprint: quant-ph/9706062.

Faugeras, O. D. and M. Hebert

1983 "A 3-D Recognition and Positioning Algorithm Using Geometrical Matching Between Primitive Surfaces", in *Proceedings of the Eighth International Joint Conference on Artificial Intelligence - Volume 2*, IJCAI'83, Morgan Kaufmann Publishers Inc., Karlsruhe, West Germany, pp. 996-1002, http://dl.acm.org/citation.cfm?id=1623516.1623603.

Fedichkin, Leonid, Dmitry Solenov, and Christino Tamon

2006 "Mixing and Decoherence in Continuous-time Quantum Walks on Cycles", *Quantum Info. Comput.*, 6, 3 (May 2006), pp. 263-276, ISSN: 1533-7146, http://dl.acm.org/citation.cfm?id=2011686.2011689.

Gebal, Katarzyna, Jakob Andreas Bærentzen, Henrik Aanæs, and Rasmus Larsen

2009 "Shape Analysis Using the Auto Diffusion Function", *Computer Graphics Forum*, 28, 5, pp. 1405-1413, ISSN: 0167-7055.

Horn, B.K.P.

1984 "Extended Gaussian images", *Proceedings of the IEEE*, 72, 12 (Dec. 1984), pp. 1671-1686, ISSN: 0018-9219, DOI: 10.1109/PROC.1984.13073.

Itano, Wayne M, Daniel J Heinzen, JJ Bollinger, and DJ Wineland

1990 "Quantum zeno effect", *Physical Review A*, 41, 5, p. 2295, DOI: 10.1103/PhysRevA.41.2295.

Johnson, A.E. and M. Hebert

1999 "Using spin images for efficient object recognition in cluttered 3D scenes", *Pattern Analysis and Machine Intelligence, IEEE Transactions on*, 21, 5 (May 1999), pp. 433-449, ISSN: 0162-8828, DOI: 10.1109/34.765655.

Kempe, Julia

2002 "Quantum Random Walks Hit Exponentially Faster", *eprint arXiv:quant-ph/0205083* (May 2002), eprint: quant-ph/0205083.

2003 "Quantum random walks: an introductory overview", *Contemporary Physics*, 44 (Apr. 2003), pp. 307-327, DOI: 10.1080/0010715103100011077 6, eprint: quant-ph/0303081.

Kendon, Viv

2007 "Decoherence in Quantum Walks - a Review", *Mathematical. Structures in Comp. Sci.*, 17, 6 (Dec. 2007), pp. 1169-1220, ISSN: 0960-1295, DOI: 10.1017/S0960129507006354, http://dx.doi.org/10.1017/S0960129507006354.

Kendon, Viv and Ben Tregenna

2003 "Decoherence can be useful in quantum walks", *Physical Review A*, 67, 4, 042315 (Apr. 2003), p. 042315, DOI: 10.1103/PhysRevA.67.042315, eprint: quant-ph/0209005.

Kuhn, Harold W

2010 "The hungarian method for the assignment problem", in *50 Years of Integer Programming 1958-2008*, Springer, pp. 29-47.

Lavallée, Stéphane and Richard Szeliski

1995 "Recovering the Position and Orientation of Free-Form Objects from Image Contours Using 3D Distance Maps", *IEEE Trans. Pattern Anal. Mach. Intell.*, 17, 4 (Apr. 1995), pp. 378-390, ISSN: 0162-8828, DOI: 10.1109/34.385980, http://dx.doi.org/10.1109/34.385980.

Litman, Roee and Alexander M. Bronstein

2014 "Learning Spectral Descriptors for Deformable Shape Correspondence", *Pattern Analysis and Machine Intelligence, IEEE Transactions on*, 36, 1 (Jan. 2014), pp. 171-180, ISSN: 0162-8828, DOI: 10.1109/TPAMI.2013.148.

Lovász, László

1993 "Random walks on graphs: A survey", *Combinatorics, Paul Erdös is eighty*, 2, 1, pp. 1-46.

Mackay, Troy D., Stephen D. Bartlett, Leigh T. Stephenson, and Barry C. Sanders

2002 "Quantum walks in higher dimensions", *Journal of Physics A Mathematical General*, 35 (Mar. 2002), pp. 2745-2753, DOI: 10.1088/0305-4470/35/12/304, eprint: quant-ph/0108004.

Majtey, A. P., P. W. Lamberti, and D. P. Prato

2005 "Jensen-Shannon divergence as a measure of distinguishability between mixed quantum states", *Phys. Rev. A*, 72 (5 Nov. 2005), p. 052310, DOI: 10.1103/PhysRevA.72.052310.

Moore, Cristopher and Alexander Russell

2002 "Quantum Walks on the Hypercube", in *Proceedings of the 6th International Workshop on Randomization and Approximation Techniques*, RANDOM '02, Springer-Verlag, London, UK, UK, pp. 164-178, ISBN: 3-540-44147-6, http://dl.acm.org/citation.cfm?id=646978.711707.

Nielsen, Michael A. and Isaac L. Chuang

2011 *Quantum Computation and Quantum Information: 10th Anniversary Edition*, 10th, Cambridge University Press, New York, NY, USA, ISBN: 1107002176, 9781107002173.

Osada, Robert, Thomas Funkhouser, Bernard Chazelle, and David Dobkin

2001 "Matching 3D Models with Shape Distributions", in *Proceedings of the International Conference on Shape Modeling & Applications*, SMI '01, IEEE Computer Society, Washington, DC, USA, pp. 154-, ISBN: 0-7695-0853-7, http://dl.acm.org/citation.cfm?id=882486.884103.

Reuter, Martin, Franz-Erich Wolter, and Niklas Peinecke

2006 "Laplace-Beltrami Spectra As 'Shape-DNA' of Surfaces and Solids", *Comput. Aided Des.*, 38, 4 (Apr. 2006), pp. 342-366, ISSN: 0010-4485, DOI: 10.1016/j.cad.2005.10.011, http://dx.doi.org/10.1016/j.cad.2005.10.011.

Rossi, Luca, Andrea Torsello, and Edwin R. Hancock

2015 "Measuring Graph Similarity through Continuous-Time Quantum Walks and the Quantum Jensen-Shannon Divergence", *Physical Review E*, To appear, ISSN: 1539-3755.

Rossi, Luca, Andrea Torsello, Edwin R. Hancock, and Richard C. Wilson

2013 "Characterizing graph symmetries through quantum Jensen-Shannon divergence", *Physical Review E*, 88 (3 Sept. 2013), p. 032806, DOI: 10.1103/PhysRevE.88.032806, http://link.aps.org/doi/10.1103/PhysRevE.88.032806.

Rustamov, Raif M.

2007 "Laplace-Beltrami Eigenfunctions for Deformation Invariant Shape Representation", in *Proceedings of the Fifth Eurographics Symposium on Geometry Processing*, SGP '07, Eurographics Association, Barcelona, Spain, pp. 225-233, ISBN: 978-3-905673-46-3, http://dl.acm.org/citation.cfm?id=1281991.1282022.

Strauch, Frederick W

2006 "Connecting the discrete-and continuous-time quantum walks", *Physical Review A*, 74, 3, p. 030301, eprint: quant-ph/0606050.

Sun, Jian, Maks Ovsjanikov, and Leonidas Guibas

2009 "A Concise and Provably Informative Multi-scale Signature Based on Heat Diffusion", in *Proceedings of the Symposium on Geometry Processing*, SGP '09, Eurographics Association, Berlin, Germany, pp. 1383-1392, http://dl.acm.org/citation.cfm?id=1735603.1735621.

Tombari, Federico, Samuele Salti, and Luigi Di Stefano

2010 "Unique Signatures of Histograms for Local Surface Description", in *Proceedings of the 11th European Conference on Computer Vision Conference on Computer Vision: Part III*, ECCV'10, Springer-Verlag, Heraklion, Crete, Greece, pp. 356-369, ISBN: 3-642-15557-X, 978-3-642-15557-4, http://dl.acm.org/citation.cfm?id=1927006.1927035.

Torsello, Andrea, Andrea Gasparetto, Luca Rossi, Lu Bai, and Edwin R. Hancock

2014 "Transitive State Alignment for the Quantum Jensen-Shannon Kernel", in *Structural, Syntactic, and Statistical Pattern Recognition*, Lecture Notes in Computer Science, Springer Berlin Heidelberg, vol. 8621, pp. 22-31, ISBN: 978-3-662-44414-6, DOI: 10.1007/978-3-662-44415-3_3, http://dx.doi.org/10.1007/978-3-662-44415-3_3.

Torsello, Andrea and Edwin R Hancock

2006 "Correcting Curvature-Density Effects in the Hamilton-Jacobi Skeleton", *Image Processing, IEEE Transactions on*, 15, 4, pp. 877-891.

Torsello, Andrea, Emanuele Rodolà, and Andrea Albarelli

2011 "Multiview registration via graph diffusion of dual quaternions", in *Computer Vision and Pattern Recognition (CVPR), 2011 IEEE Conference on*, pp. 2441-2448, DOI: 10.1109/CVPR.2011.5995565.